

N65-23741

FACILITY FORM 602

(ACCESSION NUMBER)

(PAGES)

(NASA CR OR TMX OR AD NUMBER)

(THRU)

(CODE)

(CATEGORY)

GPO PRICE \$

OTS PRICE(S) \$

Hard copy (HC)

Microfiche (MF)



Bedford, Massachusetts

SOLIDS MASS SPECTROMETER

R. F. K. HERZOG

H. J. LIEBL

W. P. POSCHENRIEDER

A. E. BARRINGTON

FINAL REPORT

CONTRACT NO. NASw-839

PREPARED FOR

NATIONAL AERONAUTICS AND SPACE ADMINISTRATION

HEADQUARTERS

WASHINGTON, D. C.

FEBRUARY 1965

GCA Technical Report No. 65-7-N

SOLIDS MASS SPECTROMETER

R. F. K. Herzog
H. J. Liebl
W. P. Poschenrieder
A. E. Barrington

FINAL REPORT

Contract No. NASw-839

February 1965

GCA CORPORATION
GCA TECHNOLOGY DIVISION
Bedford, Massachusetts

Prepared for
National Aeronautics and Space Administration
Headquarters
Washington, D. C.

TABLE OF CONTENTS

	<u>Page</u>
SUMMARY	1
INTRODUCTION	3
REDUCTION OF INSTRUMENTAL BACKGROUND	7
PERFORMANCE OF IMPROVED ION SOURCE	19
ELIMINATION OF RESIDUAL INSTRUMENTAL BACKGROUND	23
ABSOLUTE SENSITIVITY OF THE SOLIDS MASS SPECTROMETER	33
CHEMICAL TRACE ANALYSIS	35
LITHIUM ISOTOPE ABUNDANCE DETERMINATION OF THE HOLBROOK METEORITE	51
MINIATURIZATION OF THE SOLIDS MASS SPECTROMETER FOR A LUNAR MISSION	55

LIST OF ILLUSTRATIONS

<u>Figure No.</u>	<u>Title</u>	<u>Page</u>
1	Multiplier gain versus dynode-chain voltage.	8
2	Spectrum of silver target (linear peak amplitude scale) Mass 1-15.	9
3	Spectrum of silver target (linear peak amplitude scale) Mass 12-40.	10
4	Spectrum of silver target (linear peak amplitude scale) Mass 39-65.	11
5	Spectrum of silver target (linear peak amplitude scale) Mass 63-140.	12
6	Primary ion source.	14
7	Secondary ion optics.	15
8	Target holder.	16
9	Sputtering ion source.	17
10	Typical sputter craters.	20
11	Secondary ion intensity versus primary beam intensity.	21
12	Primary ion beam, oil cooled duoplasmatron (linear peak amplitude scale).	25
13	Primary ion beam, air cooled duoplasmatron (logarithmic peak amplitude scale).	29
14	Zeolite sorption pump.	32
15	Spectrum of silicon doped with 40 ppm of boron (logarithmic peak amplitude scale).	37
16	Spectrum of silicon doped with 47 ppb of boron (linear peak amplitude scale).	39
17	Boron concentration in silicon (solar cell).	40

LIST OF ILLUSTRATIONS (continued)

<u>Figure No.</u>	<u>Title</u>	<u>Page</u>
18	Boron concentration vs sputtering-time (solar cell)	41
19	Spectrum of spectroscopically pure graphite (logarithmic peak amplitude scale).	43
20	Spectrum of spectroscopically pure platinum (logarithmic peak amplitude scale).	47
21	Li-isotope ratio for Holbrook and Hornblende.	53
22	Laboratory model of solids mass spectrometer.	56
23	Proposed flight design of solids mass spectrometer.	60

SOLIDS MASS SPECTROMETER

by R. F. K. Herzog, W. P. Poschenrieder, H. J. Liebl and A. E. Barrington
GCA Corporation

SUMMARY

23741 91356
The present report deals with constructional improvements of a solids mass spectrometer and perfections in experimental technique. The improvements and perfections have resulted in a new tool with exceptionally high sensitivity for the non-destructive analysis of solids.

The methods employed for the successive reduction and final elimination of the instrumental background of the sputtering ion source and of the solids mass spectrometer are discussed in the initial sections. They include many refinements and innovations of vacuum technique; of particular importance was the utilization of spectroscopically pure structural materials in the ion source. (1)

The performance of the improved instrument is described in subsequent sections. It was possible to determine the sensitivity for the detection of trace elements with a series of doped semiconductor samples of accurately known concentrations. The purity of these materials was greatly superior to other more conventional spectrographic standards such as graphite and platinum. It was established that trace elements in the parts per billion range can be detected reproducibly and that this type of analysis is more sensitive than emission spectroscopy and neutron activation. This high level of sensitivity was achieved by means of a novel electronic memory device. The analysis of greatest interest was the determination of the isotopic abundance ratio of lithium present in the parts per million range in the Holbrook meteorite. It was possible to examine a small section of this meteorite without any previous preparation. A direct surface analysis indicated an extremely inhomogeneous distribution of lithium. Furthermore, the isotopic abundance ratio fluctuated between the wide limits of 27:1 to 9:1, whereas, the abundance ratio of terrestrial comparison samples was close to the accepted value of 12:1. This analysis conclusively demonstrated the unique capabilities of the sputter-ion technique for mass spectrometric analysis of geological specimens.

The final section deals with the design of a miniaturized solids mass spectrometer with a sputter-ion source for analysis of the lunar surface. The proposed specifications of the instrument are compatible with the payload requirements for a soft-landing lunar probe. (2)

Author

INTRODUCTION

The direct determination of the chemical composition of solids by means other than wet quantitative chemical analysis is preferred in the following cases:

- (1) When only small quantities are available for analysis.
- (2) When non-destructive analysis is necessary.
- (3) When small amounts of trace elements are present.
- (4) When the composition of surfaces and surface films is to be analyzed.
- (5) When little time is available for analysis.
- (6) When isotopic composition is of interest.

The most widely used technique is that of emission spectroscopy where the material to be analyzed is evaporated in a spark discharge and characteristic lines of the elements present are recorded on a photographic film. This method is rapid, but at best accurate down to concentrations of trace elements between one and ten parts per million. It cannot be used for surface studies and provides no information regarding isotopic composition. The requirement of the spark discharge rules out non-destructive analysis.

Surface analysis down to 100 parts per million can be performed by recording the characteristic X-ray spectrum when a surface is bombarded by a pencil of high-energy electrons. Since such an electron beam can be focussed to a diameter of the order of microns, very small areas can be illuminated in this manner. The method is non-destructive; however, the spectra can give no information about isotopic composition. The identification of light elements is complicated by the low intensity of their X-ray spectra. Furthermore, unless samples are chemically clean, spectra are confused by layers of impurities due to handling or cutting operations.

The most sensitive method which provides the maximum amount of information is mass spectrometry. Instead of the excitation of atoms and the recording of their characteristic radiation in the optical or X-ray range of wavelengths, the atoms are vaporized, ionized, and separated according to their mass-to-charge ratio. Ions of a particular species are then collected and counted.

In the conventional solids mass spectrometer, the material to be analyzed is evaporated in a spark discharge. This rules out non-destructive analysis. Furthermore, because this type of discharge is not stable, the production of ions varies with time. Thus, the intensity of a given ionic species can be measured only by using a photographic integrating technique. However, trace elements can be detected in parts per billion and accurate information regarding isotopic composition can be obtained.

The mass spectrometer principle has been extended by us so it can also be applied to non-destructive testing and to surface analysis. Instead of vaporizing the material to be analyzed in a spark discharge, the surface of the test sample is bombarded by a beam of 10 kV inert gas ions. It is well known that atoms of a surface bombarded by energetic ions are vaporized or sputtered. When the energy of the bombarding ions is sufficiently high, a significant percentage of the atoms sputtered from the surface is ionized. A portion of these ions can be focussed into a mass spectrometer analyzer and separated according to their mass-to-charge ratio. Earlier work in this area was described in the Final Reports of Contract JPL 950118 (Phase I: 31 July 1961 - 28 January 1962, Phase II: 29 January - 15 November 1962) and JPL 950576 (29 March - 30 September 1963).

The sputtering process which works with conducting and non-conducting materials results in a "peeling" of surface atoms, so that successive monolayers are sputtered and ionized. The maximum sputtering rate achieved so far is approximately 200 monolayers per second or 80 μ per hour, over an area of 0.25 mm². It is possible to enlarge the bombarded area, which, in turn, lowers the sputtering rate.

Surface ionization by sputtering has several advantages over other methods of solids analysis.

(1) No special cleaning procedure of the sample is required. Samples are introduced into an easily accessible vacuum chamber and bombarded by a beam of inert gas ions, which "cleans" off surface layers deposited by handling or cutting. Such surface layers produce spectra consisting of hydrocarbon peaks and alkali metals. Usually, such impurities are sputtered away very rapidly.

(2) Sputtering is effective for conductors and non-conductors.

(3) It is possible to study the composition of thin surface films and to determine changes of composition with depth.

(4) Because of the stability of the ion source, it is not necessary to obtain spectra by integrating with a photographic plate. Instead, the intensity of the ion current can be measured directly with an electrometer. Since the horizontal sweep of an X-Y recorder is synchronized with the current sweep of the magnetic mass analyzer, a permanent record of the spectrum is obtained.

The analytical instrument incorporating this principle consists of a primary source of noble gas ions, the target chamber, a mass analyzer, and electronic ion detector. The vacuum system consists of a well-trapped six-inch mercury diffusion pump on the target chamber. This prevents the undesirable deposition of hydrocarbon layers on the sample surface, as has been shown to be nearly inevitable when oil pumps are used. For the same

reason, the primary ion source is also pumped with a two-inch mercury diffusion pump. In order that oil contamination may be avoided when the system is roughed from atmospheric pressure, a liquid-nitrogen cooled zeolite sorption pump is used. The analyzer section is pumped by a unique combination of zeolite sorption trap and titanium sputter-ion pump, which can operate continuously for many months and results in exceptional stability of the ion detector.

The system is ready for operation about 10 minutes after the sample is introduced in the target chamber, which is readily evacuated below 10^{-6} Torr. A low voltage arc is then initiated in the ion source which is maintained at about 10^{-2} Torr from a noble gas reservoir (Argon, Xenon, etc.). The arc is strongly constricted by an axial magnetic field, so that a very dense plasma is created along the axis near the anode. Through a pinhole in the anode, an intense beam of noble gas ions is extracted and accelerated by a conically shaped electrode. In this manner, an ion beam of about 1 ma of small cross-sectional area is obtained. The beam bombards the target at an oblique angle of incidence - this causes a higher rate of sputtering than normal impact. Because the bombarding beam consists of ions of a chemically inert gas such as argon, no chemical reaction occurs and the target remains uncontaminated.

The secondary ions of surface material produced in this manner are focussed electrostatically into a double-focussing mass spectrometer where they are separated in a magnetic sector according to their momentum-to-charge ratio and are subsequently sorted according to their energy by an electrostatic analyzer. The intensity of the ion current corresponding to a given mass peak is measured electronically. A spectrum is obtained when the potential through which the surface ions are accelerated is changed or when the magnitude of the magnetic field at constant ion accelerating potential is changed. A permanent record of the spectrum is obtained by synchronizing the horizontal sweep of an X-Y recorder with the parameter varied and making the vertical deflection proportional to the ion current. A linear or a logarithmic read-out is available; the logarithmic scale covers over six orders of magnitude. Trace constituents in parts per million can then be recorded directly. For smaller concentrations, it is necessary to utilize a Digital Memory Oscilloscope. It extends the sensitivity of the instrument by at least two orders of magnitude.

In order to achieve this performance which was the goal of the present investigation many innovations had to be made. These include advances in vacuum technique, refinements of the gas inlet system and of the inert-gas ion source, and the use of recording techniques utilizing the above mentioned electronic memory device.

Numerical values of the detection limit were determined from spectroscopically pure materials with accurately known trace impurities in the parts

per billion range. A most useful material, and at present the only one to satisfy these stringent requirements, is high-purity silicon doped with boron.

The major portion of the present report deals with details of instrumental technique and includes many novel experimental data.

On the basis of the wide experience gained with the present instrument, a design for a lunar surface analyzer is proposed in the final section. The analyzer would perform in-situ analysis of the lunar surface.

REDUCTION OF INSTRUMENTAL BACKGROUND

As stated in the Final Report of JPL Contract 950576, the instrumental performance of the sputtering source solids mass spectrometer showed great promise for trace analyses. However, full understanding of the behavior of the ion source and an evaluation of the overall sensitivity of this analytical method were not possible because the instrumental background was too high. One of the major objectives of the present investigation was the reduction and, if possible, total elimination of this background.

Background Spectra with Electron Multiplier

In order to improve the sensitivity of the existing mass spectrometer for trace analysis, we equipped the mass analyzer with a twenty-stage electron multiplier of the Van Allen type. Figure 1 shows a plot of multiplier gain versus voltage across the dynode chain, using an input current of 5×10^{-14} A of Al^+ ions.

Figures 2 to 5 show secondary ion spectra obtained from the bombardment of a silver target with argon ions. The impurities of the target were certified to be less than 1 ppm. The multiplier gain was 10^5 . The output of the multiplier was fed into a vibrating reed electrometer; the output voltage of the electrometer was displayed as the Y-coordinate of an X-Y recorder. The spectra cover the mass range up to approximately 160 AMU. The secondary ion accelerating field and the electrostatic deflecting field were scanned proportionally to cover the mass range. Since the X-coordinate of the recorder trace is proportional to the secondary ion acceleration voltage V , the mass scale increases from right to left according to the expression $MV = \text{constant}$, which holds for all ions of mass M moving along the same path in a constant magnetic field. Further, the sensitivity decreases from right to left, since the ion collection efficiency decreases as the ion accelerating voltage is reduced during the scan.

The background peaks appearing on the spectra can be considered typical. Many peaks are easily identified, such as the elements C^+ , Na^+ , Mg^+ , Al^+ , Si^+ , K^+ , Fe^+ , Cu^+ , and, of course Ar^+ and Ar^{2+} .

The identity of the majority of the background peaks, however, remains uncertain; they most likely are fragmentation products of various hydrocarbon molecules which stem from the pump oil or from grease in the gas inlet system carried along with the argon.

Regarding the distinct elemental impurity peaks, it must be assumed that they arose from deposits on the target surface. Such deposits must be expected if other surfaces in the ion source are bombarded by the primary beam causing sputtering and if some of this sputtered material is deposited on the target.

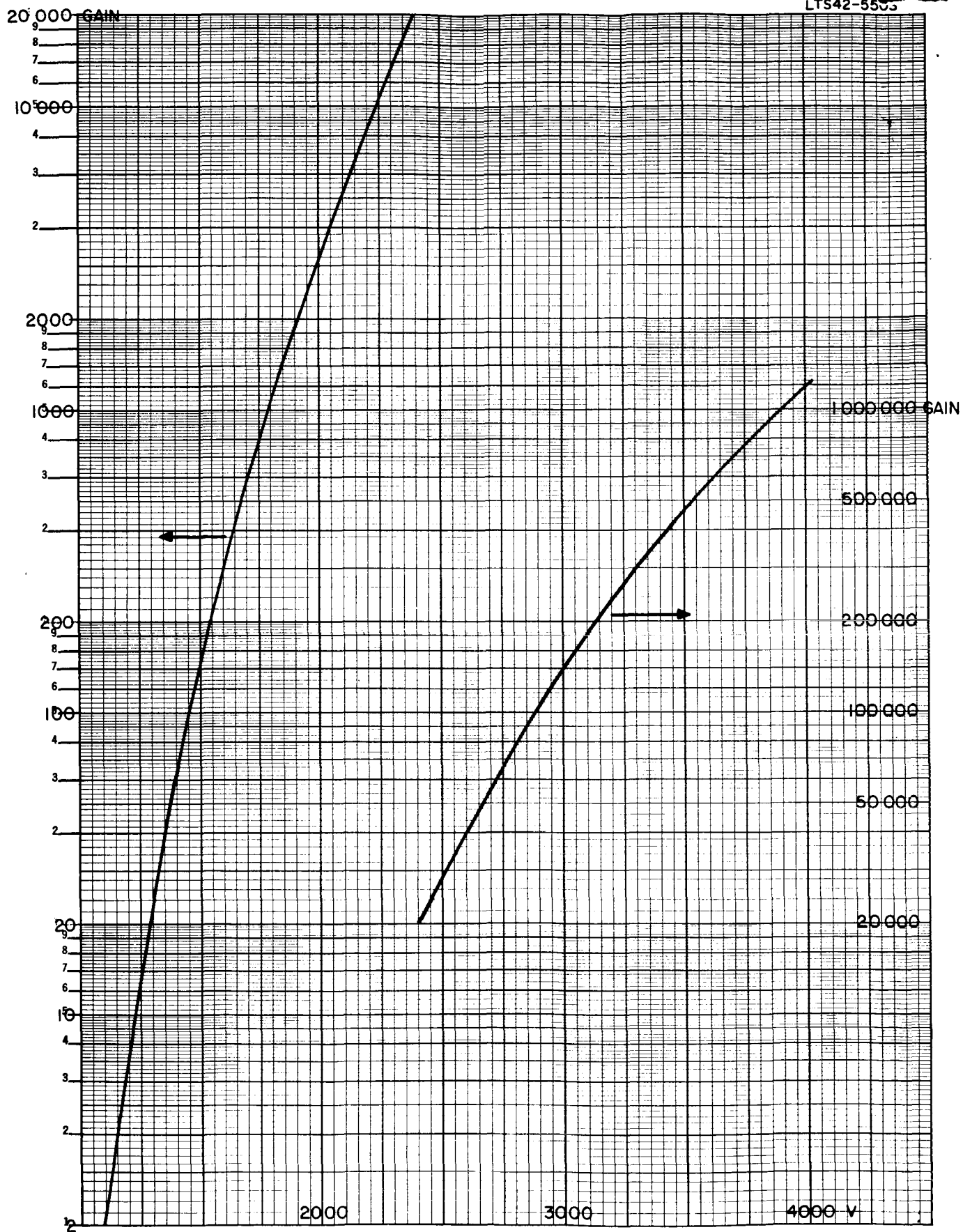


Figure 1. Multiplier gain versus dynode-chain voltage.

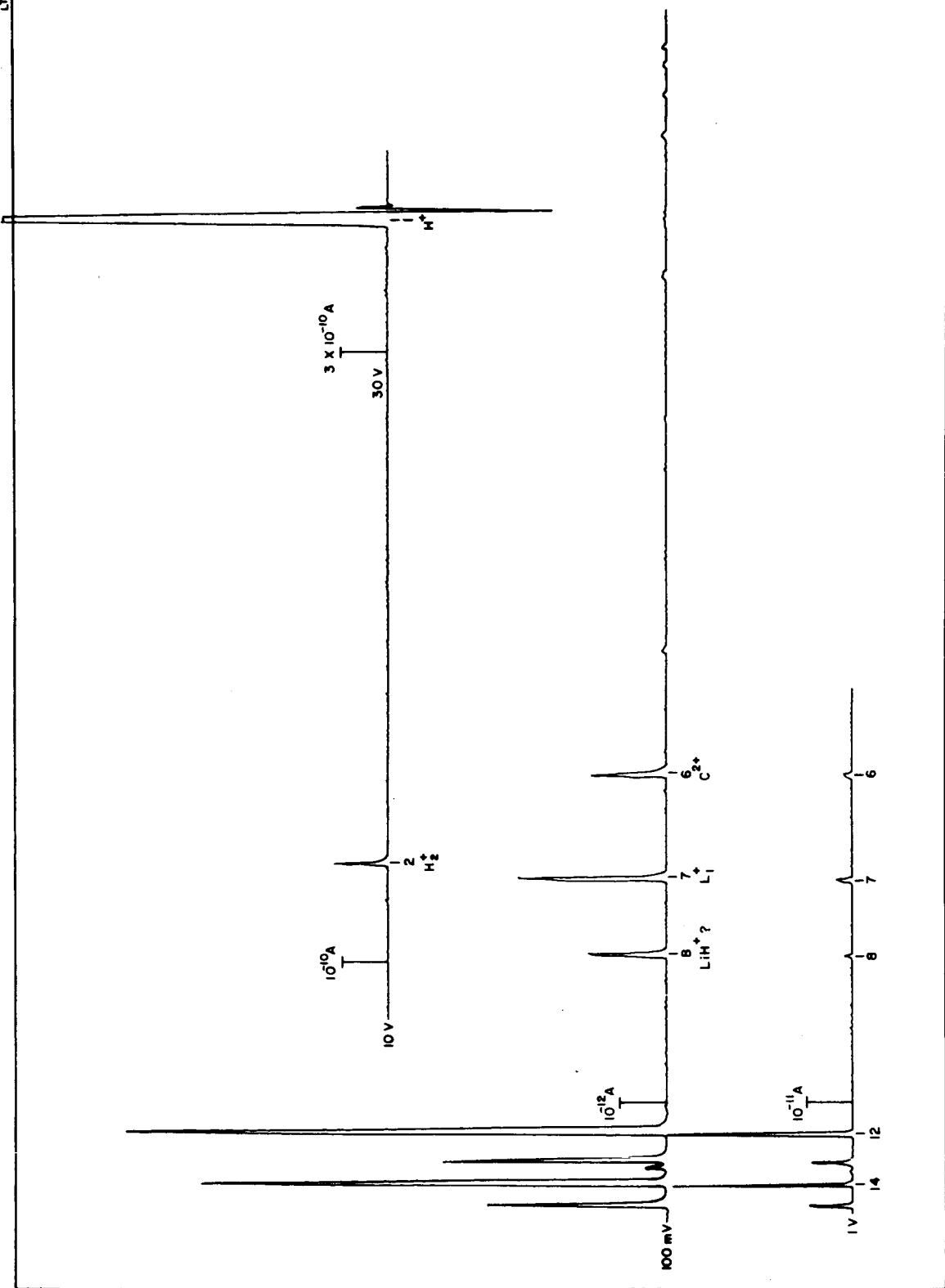


Figure 2. Spectrum of silver target (linear peak amplitude scale) Mass 1-15.

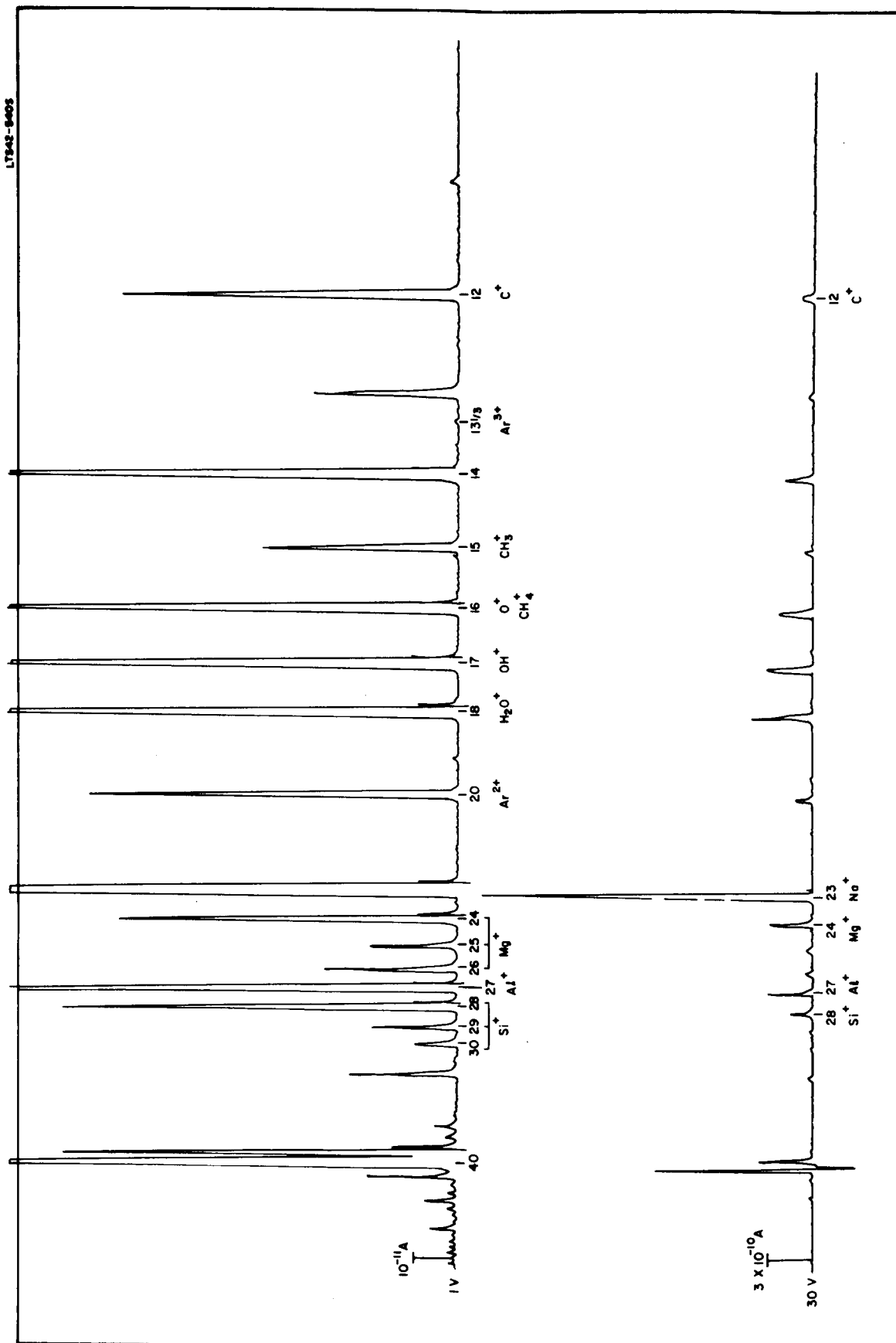


Figure 3. Spectrum of silver target (linear peak amplitude scale) Mass 12-40.

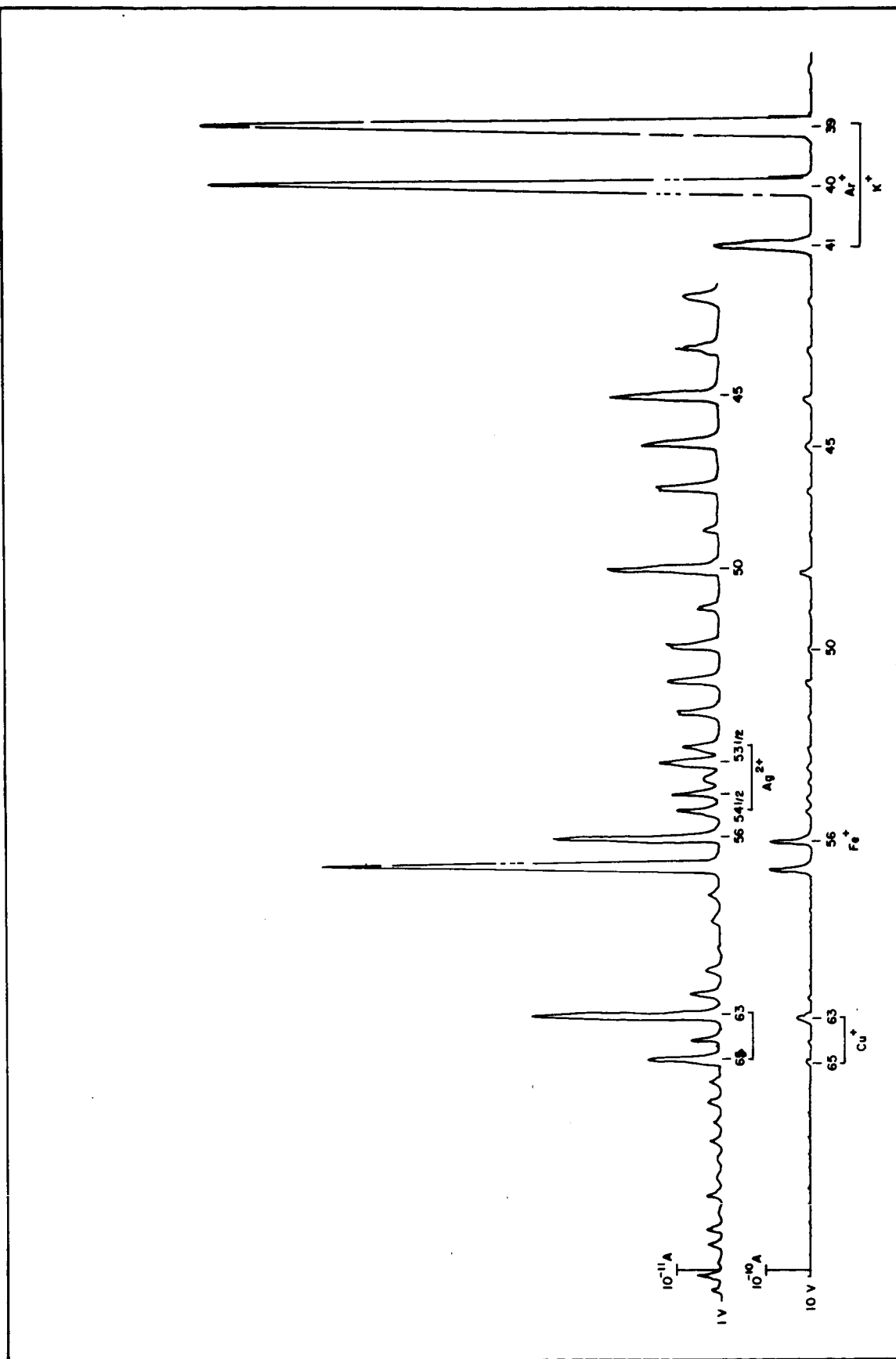


Figure 4. Spectrum of silver target (linear peak amplitude) Mass 39-65.

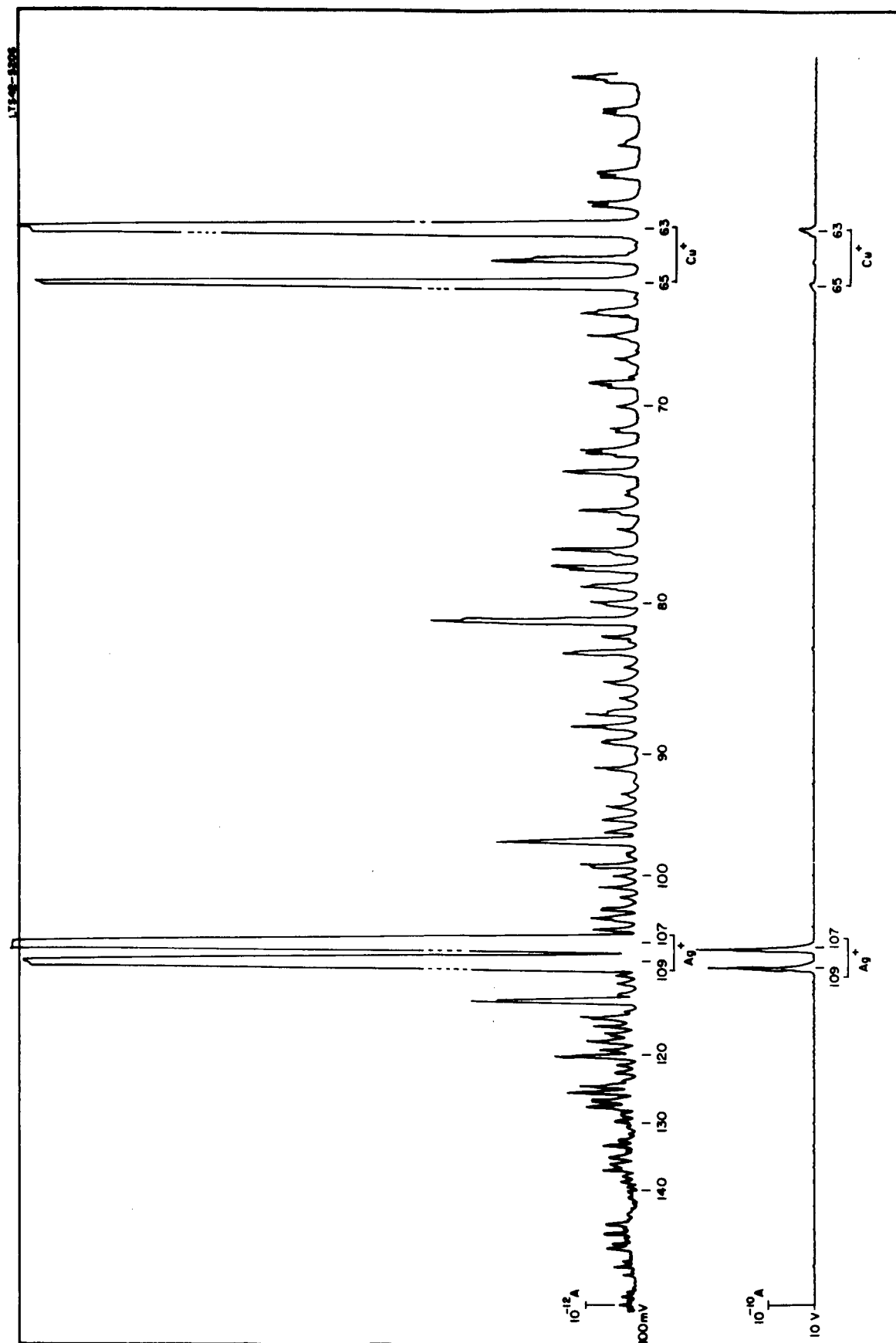


Figure 5. Spectrum of silver target (linear peak amplitude scale) Mass 63-140.

Reduction of the background required several corrective steps. These included the rebuilding of the ion source with spectroscopically pure materials and improving the ion optics, eliminating the sources of hydrocarbons in the pumping system and in the gas inlet system, and improving the manipulation procedure of the targets.

Improvements of Ion Source

Parts in contact with or close to the primary ion beam are the duoplasmatron anode which carries the extraction orifice, the apex of the ion extraction and accelerating electrode, the aperture plate at the exit of the einzel lens, the beam adjustment plates and the target electrode (Figures 6 and 7). Tantalum was chosen for these parts because its high mass number (181-abundance 100%) causes little interference with other mass peaks, because it has a low sputtering efficiency and because it is available in high purity. The atomic mass of the tantalum ion and its polymers is well beyond the mass range of greatest interest.

Replacing the plexiglass insulation flange between the duoplasmatron and the main housing by a flange of pyrex glass avoided another possible background source.

The primary ion optics was designed for a smaller spot size and better adjustability. Two of the three electrodes of the einzel lens are adjustable by fine screw threads for precise axial adjustment of the focal spot on the target. In addition, two pairs of mutually perpendicular plates mounted at the exit of the einzel lens permit transverse adjustment of the beam. (See Figure 6.)

The targets to be analyzed are mounted on a tantalum bar containing 0.1% niobium as the major impurity (which is readily detected during a sputter analysis). The bar is attached to a ceramic bushing which is welded to the outer of two concentric stainless steel tubes. A drive nut provides axial motion and two crossed dovetails provide transverse motion. A flexible vacuum seal is provided by a welded stainless steel bellows. The target may be cooled by a fluid which flows in the two concentric tubes (Figure 8), however, this has not been found to be necessary.

A viewing port permits observation of the primary beam; while under ion bombardment, the target surface can be inspected through a mirror arrangement and a telescope. The ion source assembly is shown in Figure 9.

All greased stopcocks were eliminated from the gas inlet system. The argon passes through a liquid nitrogen trap before it is admitted through a micrometer-controlled metering valve into the duoplasmatron.



Figure 6. Primary ion source.

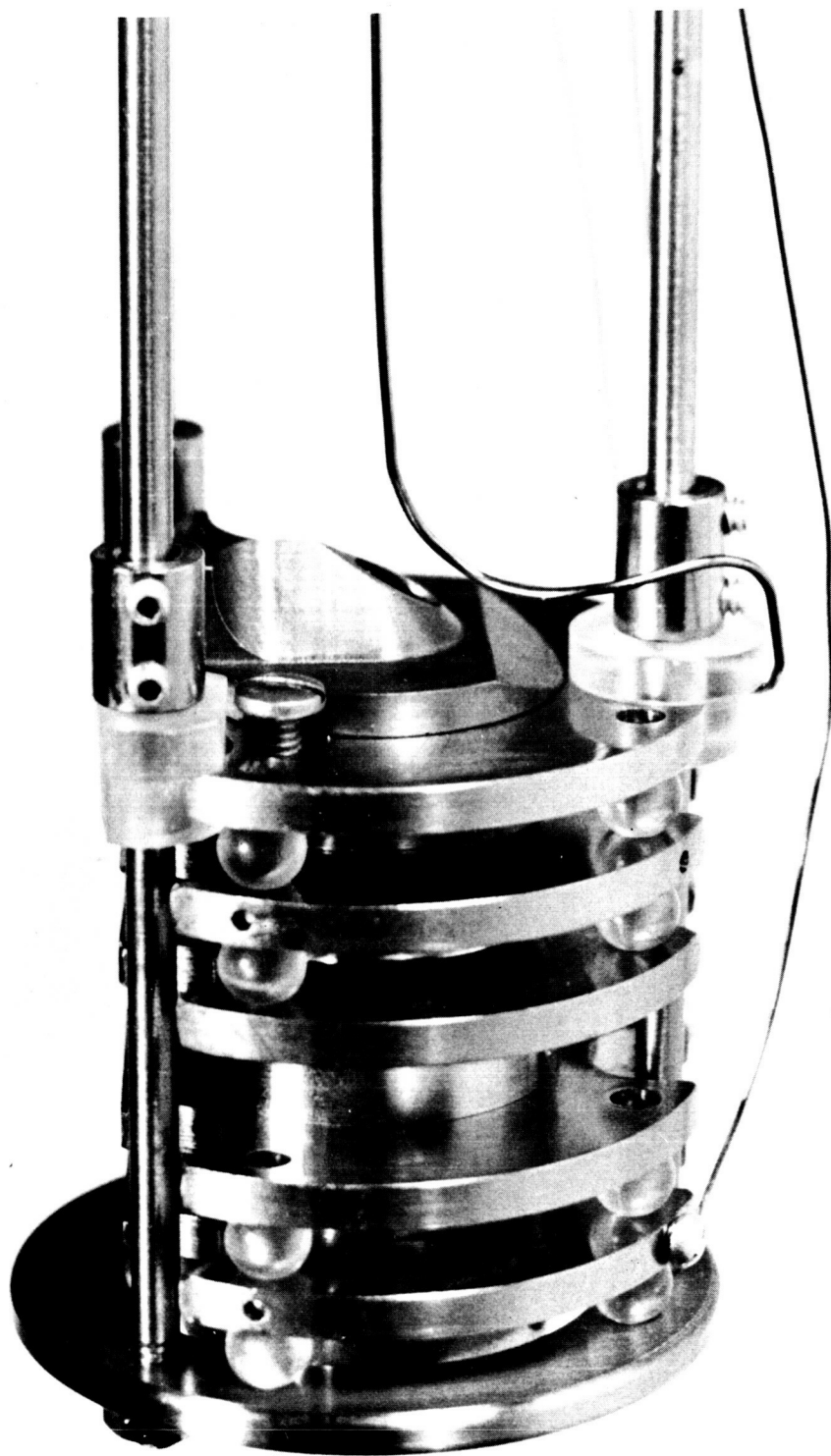


Figure 7. Secondary ion optics.

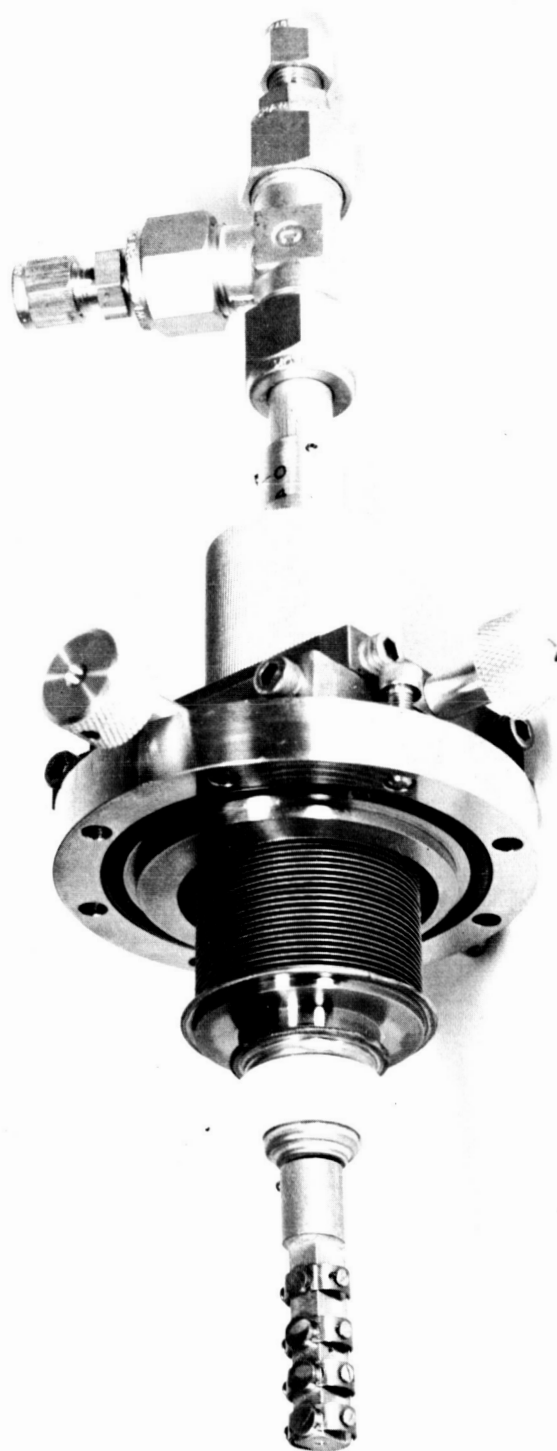


Figure 8. Target holder.

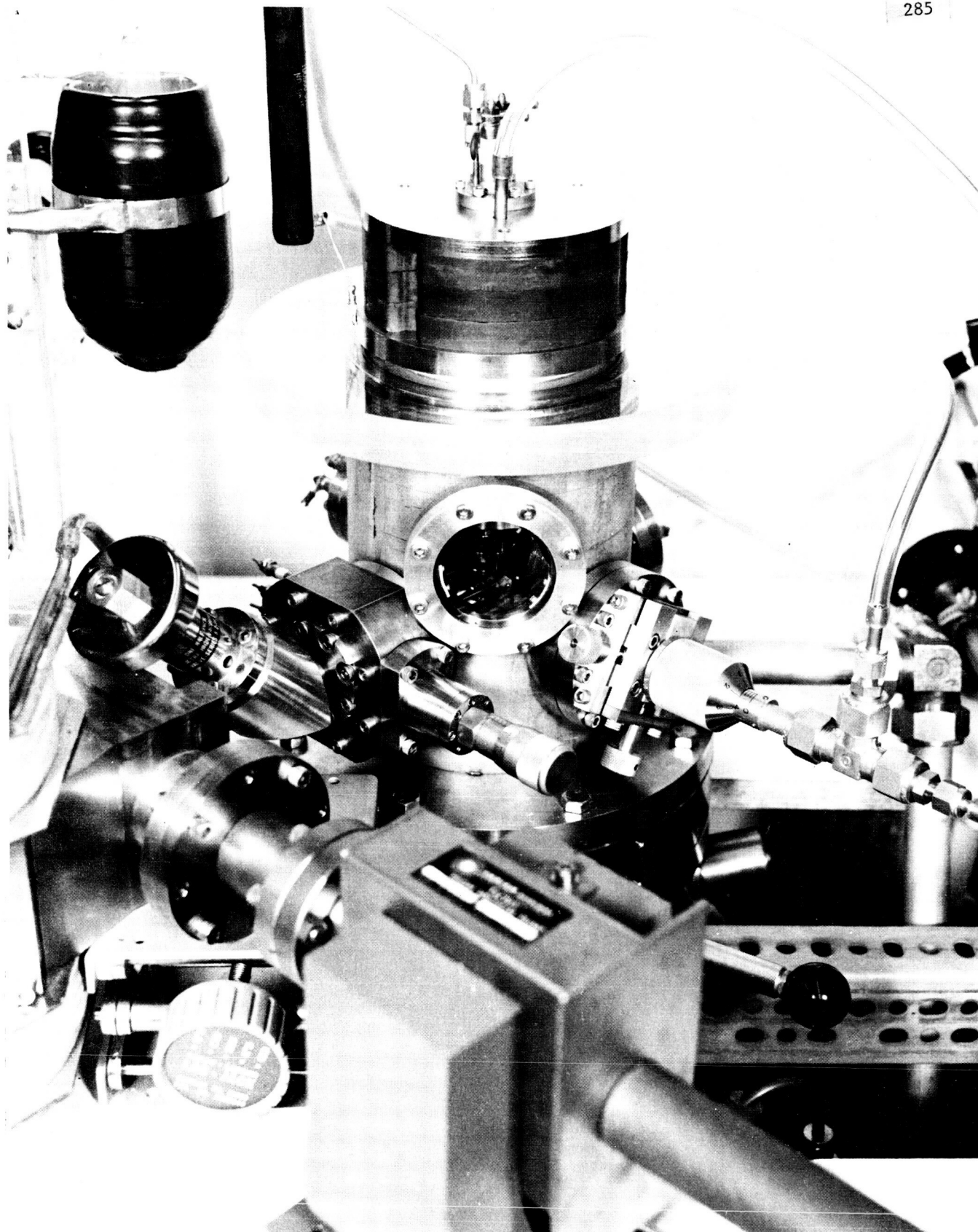


Figure 9. Sputtering ion source.

Improvement of the Vacuum System

The vacuum system was rebuilt with a 6-inch mercury diffusion pump trapped with a liquid-nitrogen cooled baffle. A butterfly valve was installed above the liquid-nitrogen baffle. Targets can now be changed readily by closing the butterfly valve and venting the system to an atmosphere of dry nitrogen. The mercury pump is backed by a mechanical forepump. As constructed initially the target chamber could be rough-pumped by the mechanical forepump via a by-pass line. Since this procedure leads to contamination by forepump oil, rough-pumping of the target chamber and duoplasmatron ion source is now performed by a valveable zeolite forepump.

The mass analyzer was equipped with two 15 liter/sec sputter-ion pumps. Since the analyzer can be valved off from the target chamber during target changes, it never is exposed to atmospheric pressure at any time. The ion pumps operate continuously and maintain the pressure in the analyzer below 10^{-7} Torr.

PERFORMANCE OF IMPROVED ION SOURCE

Arranging the two outer electrodes of the electrostatic einzel lens so that the smallest image is produced with the center electrode at the full potential of the duoplasmatron anode simplified the power supply for the primary beam. The center electrode can thus be connected internally to the duoplasmatron anode. With an acceleration voltage of 10 kV, the diameter of the image on the target is 0.3 mm, which is the theoretical minimum. The diameter of the ion exit hole in the duoplasmatron anode is 0.25 mm and the imaging ratio equals 1:1.2.

Figure 10 shows several targets after prolonged bombardment with a 10 kV, 50 microamperes beam of argon ions. The angle of incidence at the target was 30° . The silver sample was bombarded for $2\frac{1}{2}$ hours, resulting in a tapered hole, 0.5 mm deep. The cadmium sample was bombarded near the edge for $1\frac{1}{2}$ hours and was penetrated by the beam. The tantalum and copper targets were bombarded intermittently at various surface locations, the copper target for about one hour, the tantalum target for several hours.

Although the samples were not cooled during these runs, even with the low melting cadmium (321°C) no melting has occurred, since the edges and walls of the hole have a sharp and crystalline appearance, unlike that of metal solidified from the liquid state. This is also illustrated by the furrows visible on the sputtered copper surface. As was to be expected, the tantalum had a much lower total sputtering yield than the other metals.

The spot on the target can be moved from the axis in either direction over about one mm with the two pairs of mutually perpendicular deflection plates which the primary beam passes after the einzel lens. This adjustment is used in practice to line up the spot with the axis of the secondary ion optics, in order that the maximum yield of the mass analyzer may be obtained. The target can be moved during operation perpendicular to its surface, which permits compensation for different target thicknesses, and in two mutually perpendicular directions parallel to its surface, which facilitates exposing different areas of the surface to the primary beam.

The beam intensity can be varied between 30 μA and 120 μA by variation of the arc supply voltage. The secondary ion intensity follows the variation of the primary beam intensity in an essentially linear manner, as can be seen in Figure 11. This is in contrast to a hypothesis that the secondary ions might be formed by ionization of sputtered neutrals by the primary beam, which would call for a square law dependence of the secondary ion intensity from the primary beam intensity. The curve actually slopes the opposite way, which could be the result of beam spreading with higher intensity.

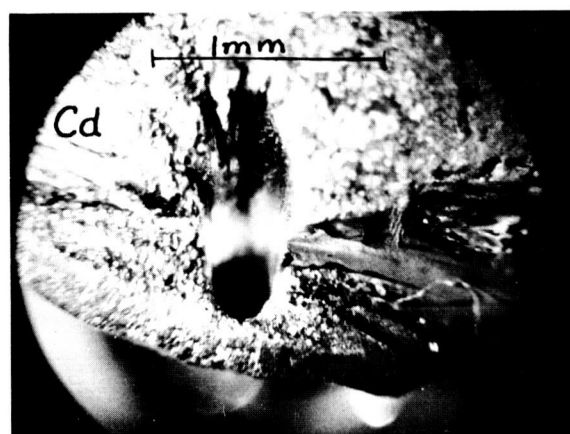
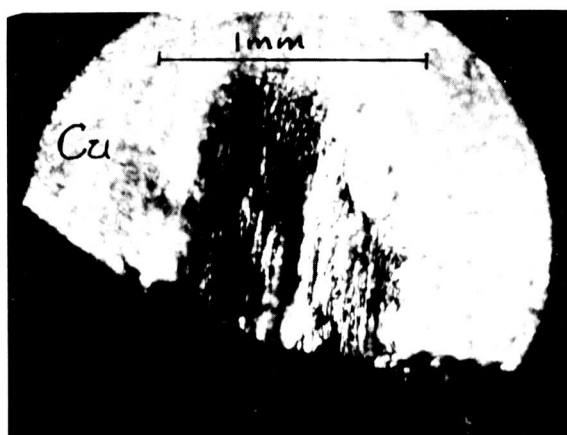
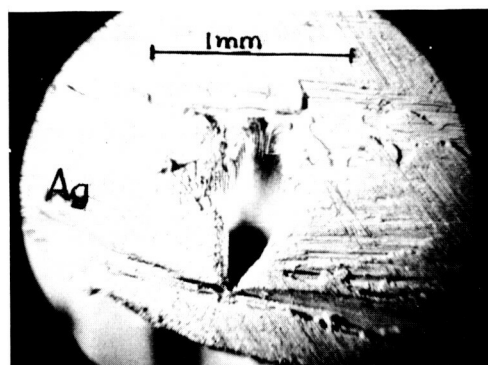
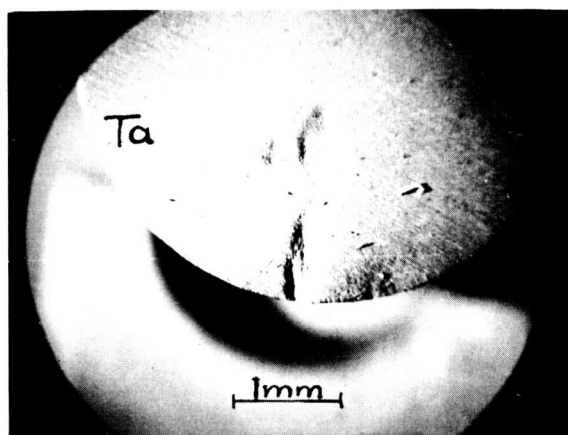


Figure 10. Typical sputter craters.

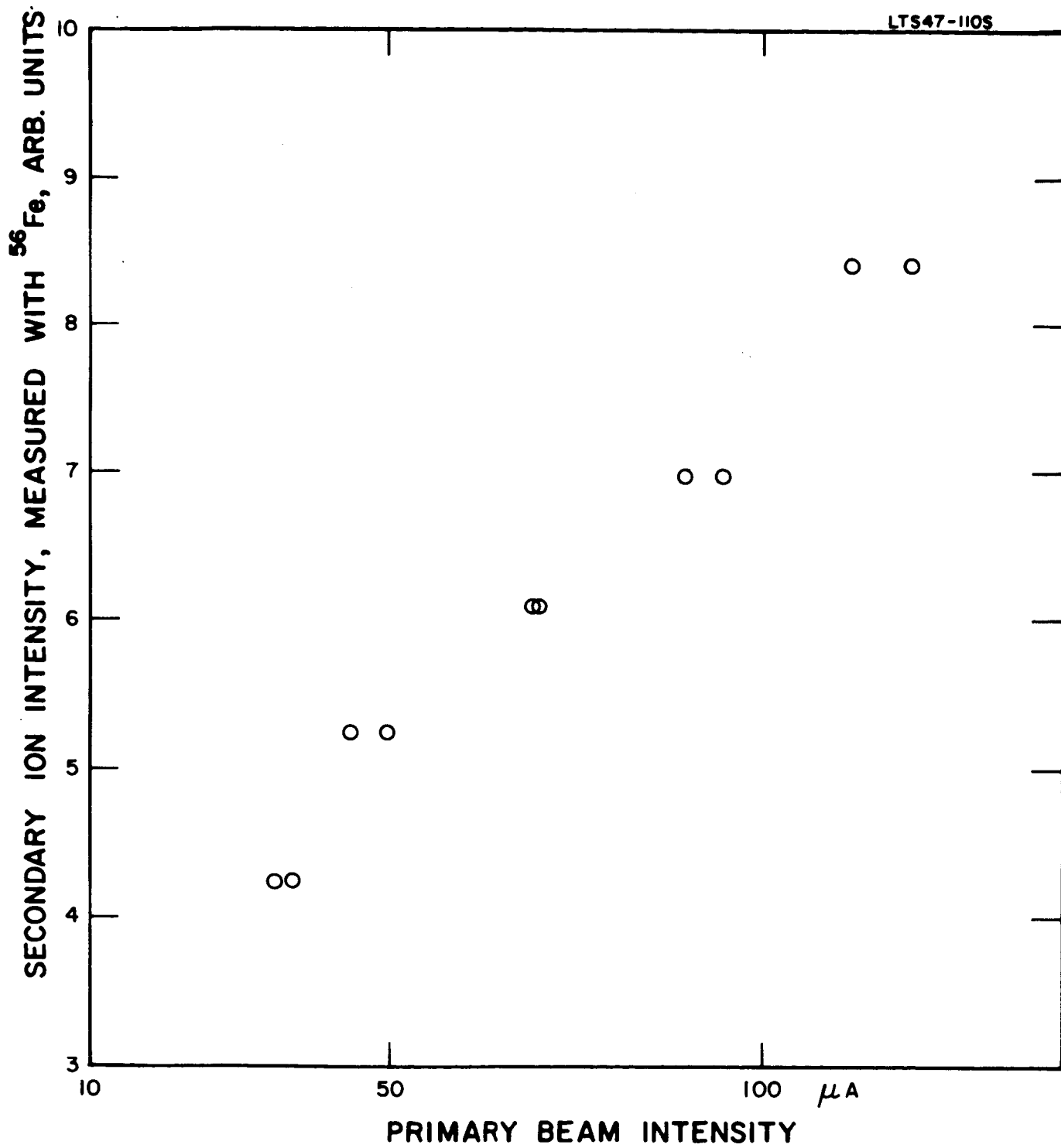


Figure 11. Secondary ion intensity versus primary beam intensity.

ELIMINATION OF RESIDUAL INSTRUMENTAL BACKGROUND

Following the improvements in the Ion Source and the installation of a vacuum system free of organic pumping fluids, the instrumental background was reduced sufficiently so that trace elements in the parts per million range could be detected for the first time. However, the background spectrum still contained several unexplained mass peaks and base-line instabilities. The identification of the sources of this residual background and the various steps taken for its elimination constituted a major effort during the program.

Primary Ion Beam

In order to produce clean spectra from targets by inert-gas ion bombardment, it is essential that the primary high-energy ion beam is free of contaminants. Unless this condition is fulfilled, it is possible for such contaminants to be sputtered and ionized together with the target material. Since these contaminants have to be excluded from the trace analysis, it is of prime importance to have the primary beam as pure as possible.

The composition of the primary beam can be examined by the following method. After adjustment of all the controls for maximum output of the main target peak, the mass analyzer is tuned to the mass 40 peak of argon. Then the primary beam accelerating voltage is reduced until the output shows a sharp maximum. This happens, when the primary beam voltage equals the target voltage, because then the field in front of the target acts as an "ion mirror" and reflects the ions. A good fraction of the ions are accelerated by the secondary ion optics and analyzed in the mass spectrometer.

The primary beam delivered by the oil-cooled duoplasmatron showed many background peaks (Figure 12), mainly hydrocarbons. A close inspection of the duoplasmatron after prolonged operation revealed the following situation: The circular channel which carried the coolant was sealed against the arc chamber by two Viton "O"-rings which were compressed between a smooth metallic and a polished ceramic surface (See Figure 1 of Final Report Contract No. 950576). Even though these seals are vacuum tight, as tested with a helium leak detector, they did not prevent the transformer oil, used as coolant, from creeping through into the arc chamber. A radical remedy for this situation was the replacement of the oil-cooled duoplasmatron by an air-cooled version of otherwise very similar construction. The hydrocarbon background was greatly reduced thereby, and above mass 65, completely eliminated.

The next suspect responsible for the remaining impurities in the primary beam was the filament. The filaments were fabricated from platinum mesh (.004 inch wire) which was cut into $\frac{1}{4}$ -inch by 2-inch strips, rolled up, soaked in the chemical R-500, a suspension of barium carbonate in n-butyl acetate and n-butyl alcohol, dried, and then activated by heating in vacuum, which reduces the barium carbonate to barium oxide and supposedly decomposes the organic binder. It was suspected that this type of filament continued to release hydrocarbons after activation, and that the barium contained such impurities as sodium and potassium which appeared in the spectrum.

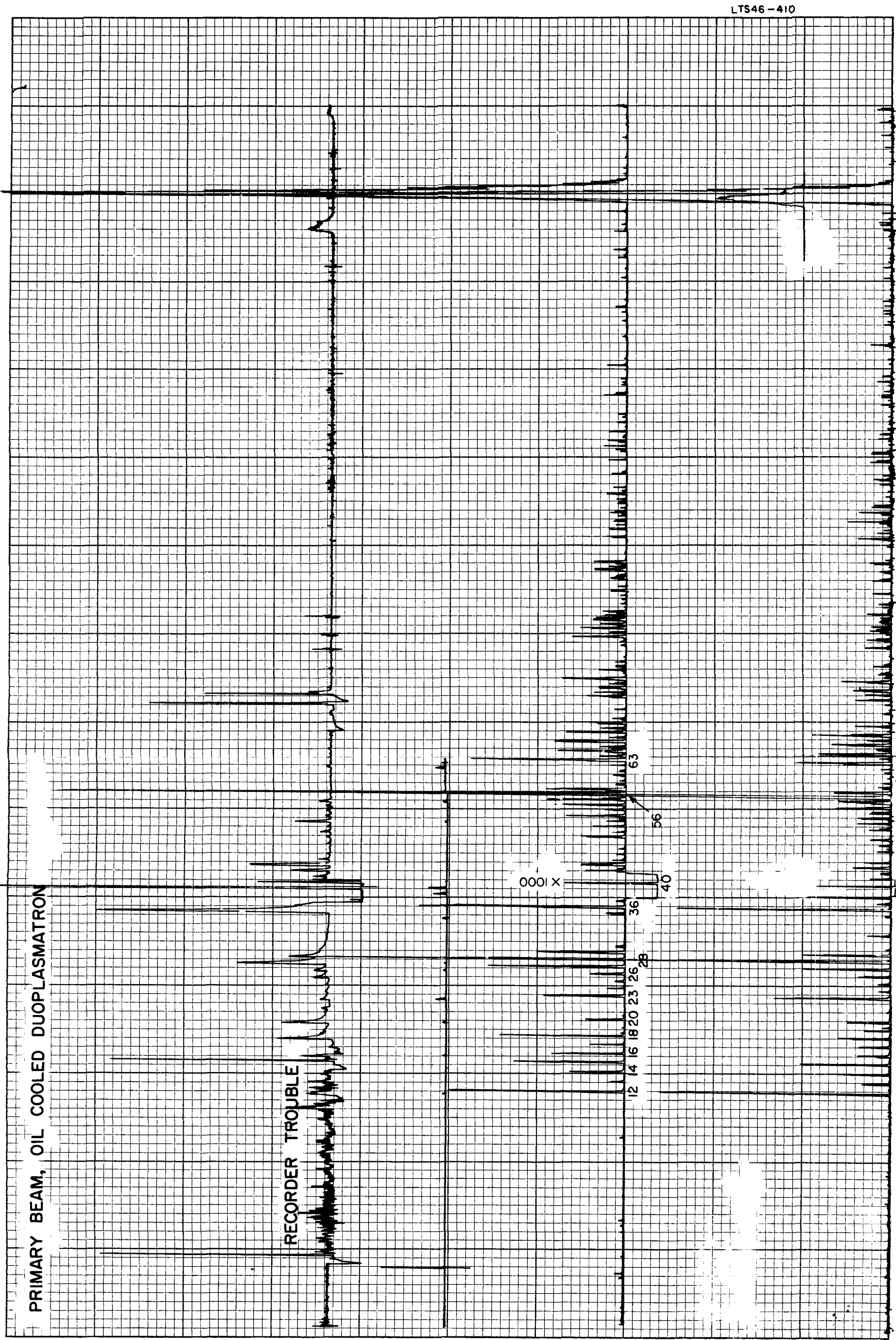


Figure 12. Primary ion beam, oil cooled duo-plasmatron (linear peak amplitude scale).

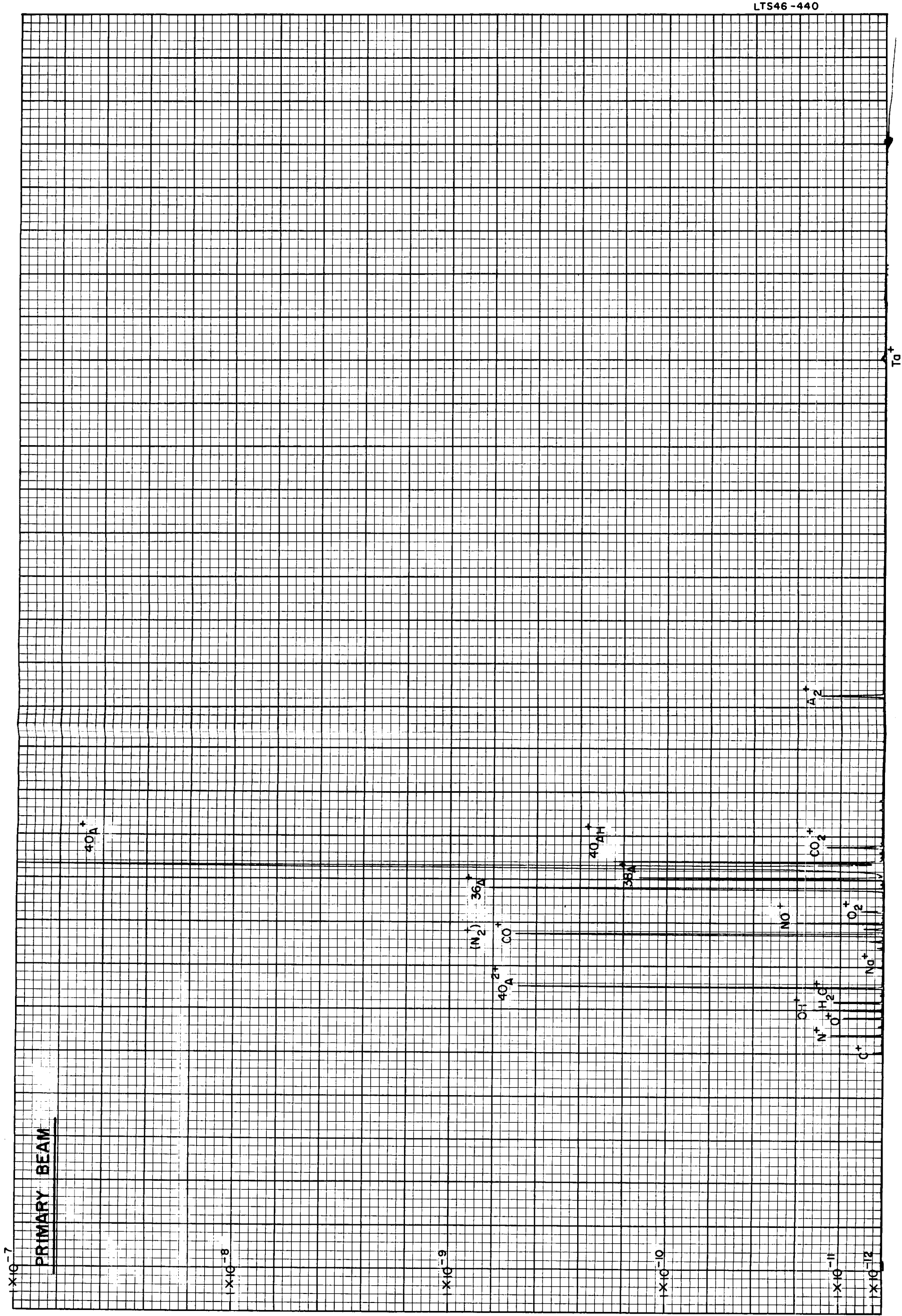
Consequently, this filament was replaced by a tungsten wire containing 2% thorium. Further, in order that the strong iron and copper peaks be eliminated, the baffle electrode was lined with a thin-wall tantalum insert, and the anode was modified, such that all the walls in contact with or close to the arc are constructed of tantalum. The tungsten filament caused a significant reduction in the peak heights of low-mass hydrocarbon peaks. Although the tungsten filament operates at a higher temperature than the platinum mesh cathode, its life extends over many weeks, provided it is not exposed to oxygen when hot.

The final step in obtaining a pure primary beam was the modification of the manner for the evacuation of the duoplasmatron. Initially, pumping was possible only via the ion beam exit hole of 0.25 mm diameter and consequently, the argon flow was very slow. To increase the proportion of argon over possible impurities we added a manifold for differential pumping by a liquid-nitrogen trapped 2-inch mercury diffusion pump. In this manner, the argon flow was increased by a factor of 50.

The resulting spectrum of the primary beam is shown in Figure 13. Since we are dealing with an unbaked gas inlet system, water vapor has to be expected as the major contaminant. In fact, however, the H_2O^+ and OH^+ peaks are extremely small. It appears that the water vapor is dissociated; the oxygen combines with carbon, presumably at the hot tungsten filament to form CO^+ (the major contaminant peak) and CO_2^+ . The hydrogen appears in a combination with argon as the molecular ion AH^+ . There is practically no indication of any hydrocarbon contamination left. The peak at mass 15 (CH_3^+) which is normally a strong peak in most hydrocarbon spectra, is almost six orders of magnitude smaller than the peak at mass 40 (A^+). Apart from Ta^+ , the structural material of the duoplasmatron, and small traces of carbon, oxygen and nitrogen, which may be present in the commercial High-Purity argon or be released by the structural materials, no other elemental peaks are present. The gaseous contaminants in the primary beam amount to only about one part in 10^4 ; their contribution to the secondary spectrum is further reduced by several orders of magnitude.

Vacuum System

It had been anticipated that the replacement of the oil diffusion pumps by sputter-ion pumps could create a problem in that charged particles and ultraviolet light could escape from the Penning-type discharge in the pumps and introduce noise in the multiplier. Care had been taken, therefore, to connect these pumps at an angle with the analyzer housing and to install an optical baffle so that there was no direct optical path between the pumping ports and the multiplier input. Nevertheless, it turned out that the operation of these pumps did introduce noise in the multiplier. This happened not only with the pump mounted close to the multiplier, but even with the second pump mounted on the opposite end of the analyzer in which case ions are deflected and neutral particles or photons have to collide many times with the walls of the apparatus in order to reach the multiplier.



K&E 5 X 5 TO THE 1/2 INCH 358-6L
KEUFFEL & ESSER CO. MADE IN U.S.A.

Figure 13. Primary ion beam, air cooled duoplasmatron (logarithmic peak amplitude scale).

The background signal was not affected by the strong magnetic field (up to 12,000 gauss) which is located between the sputter-ion pump and the multiplier. It was suspected that the noise was produced by photons from decaying metastable atoms which have a sufficiently long lifetime to diffuse into the multiplier section. One immediate remedy was to shut off the sputter-ion pumps during an experimental run. However, this procedure resulted in an undesirable pressure increase in the analyzer section, which ultimately resulted in malfunctioning of the multiplier.

Adequate pumping during runs without electrical interference was obtained with a zeolite sorption pump (Figure 14) constructed with two ports fitted with flanges profiled for bakeable copper shear-seals. One port was connected to a sputter-ion pump (15 liters/sec), the other to a $1\frac{1}{2}$ -inch valve with a Viton-A seat.

The zeolite-pump sputter-ion pump combination was first evacuated by a well-trapped mechanical pump to less than 10^{-4} Torr. The zeolite temperature was then raised to 350°C with a simple immersion heater placed in the well provided as a liquid nitrogen reservoir. Evacuation continued until the pressure, with the zeolite hot, fell below 10^{-3} Torr. The zeolite-pump sputter-ion-pump combination was then valved off and disconnected from the exhaust manifold. The pressure decreased to less than 10^{-5} Torr when the zeolite cooled to room temperature, and to below 10^{-7} Torr when chilled to liquid nitrogen temperature.

The zeolite pump was then connected to the mass spectrometer analyzer, but the connecting valve was not opened until the analyzer section was evacuated by the other pumps (mechanical forepump, mercury-diffusion pump and 15 liter/sec sputter-ion pump) to less than 10^{-6} Torr.

Initially, the zeolite pump was operated at liquid nitrogen temperature, with the sputter-ion pumps shut-off during a run. As expected, the noise in the multiplier was negligible and thus the sensitivity of the machine was greatly improved. The chilled zeolite pump is effective for all gases except hydrogen, helium, and neon; it is thus entirely suitable for the heavier noble gases such as argon, krypton and xenon which are used to bombard the targets to be analyzed.

It was suspected, however, that the zeolite might be effective in preventing metastable atoms produced by the discharge in the sputter-ion pump from reaching the analyzer. This turned out to be the case and it is now possible to perform experiments without disconnecting the sputter-ion pump.

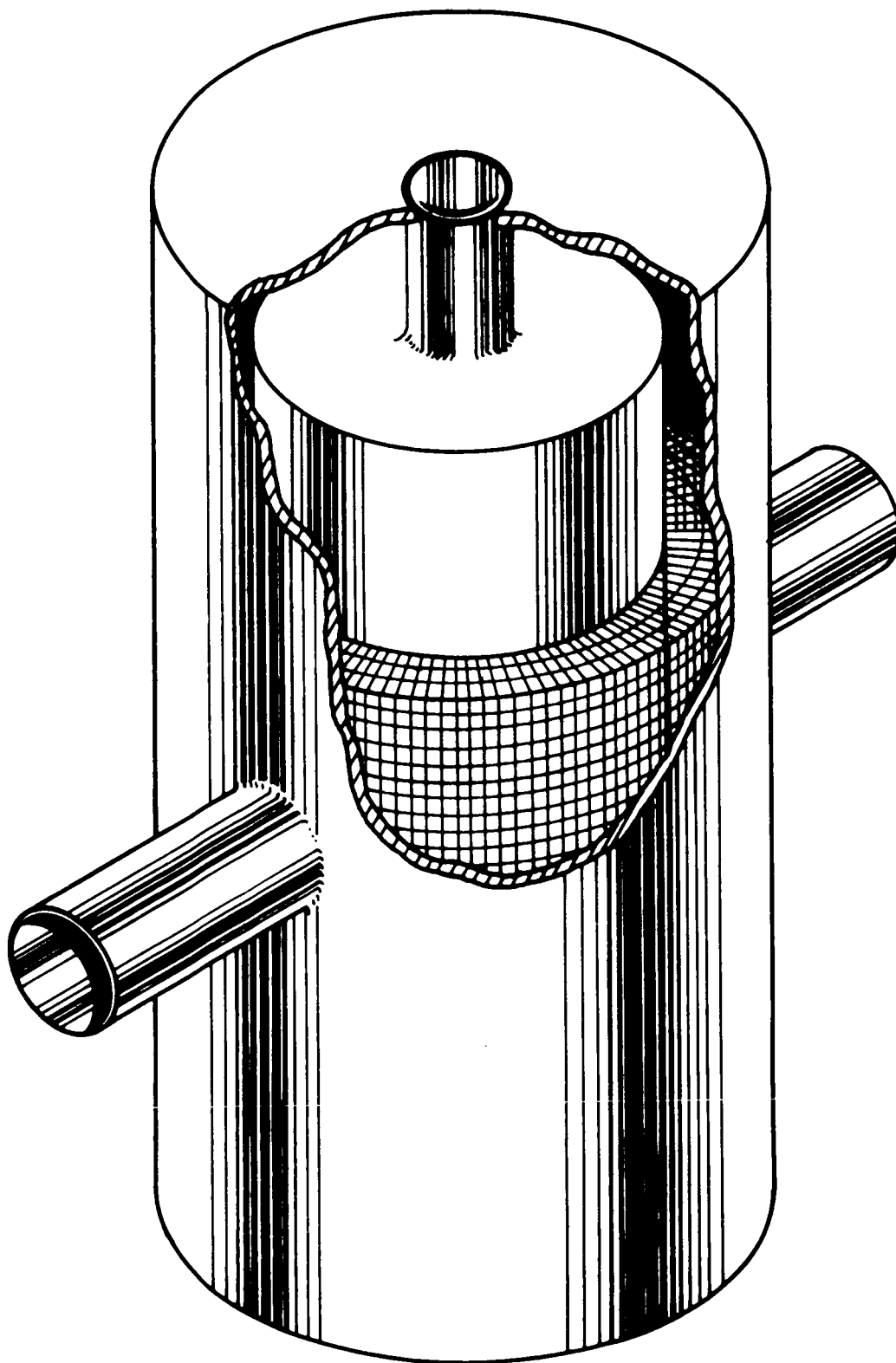


Figure 14. Zeolite sorption pump.

ABSOLUTE SENSITIVITY OF THE SOLIDS MASS SPECTROMETER

In order to use the instrument for quantitative chemical analysis, it is necessary as a first step to measure the relative ion yield of pure elements under bombardment by ions of suitable gases under otherwise identical conditions.

The ion yields of the pure metals listed in Table I were measured under bombardment with 8 kV Xenon ions and 8 kV Argon ions. A set of three samples was always mounted together with one tantalum sample. The ion yield from the tantalum sample was taken as a standard. The effect of variations of the primary beam intensity was eliminated by relating the peak heights of the three samples to that of tantalum. The primary beam was kept on while changing from one sample to the next, and the samples were adjusted for maximum ion yield.

Table I

	8 kV Xe ⁺	8 kV Ar ⁺
Mg	20.9	107
Al	7.2	790
Fe	4.2	22.6
Co	1.5	3.2
Ni	1.68	1.8
Cu	.79	2.4
Zn	.95	3.2
Zr	.56	3.0
Nb	.09	3.7
Ag	.01	.94
Cd	.38	.11
In	1.67	5.0
Sn	.72	
Ta	1	1
Au	.006	.008
Pb	3.0	4.2

Comparison between the results from Xe^+ and Ar^+ bombardment shows that, in general, the spread in the sensitivities, or the so-called discrimination factor, is smaller for the heavier bombarding ion. This can be an advantage or disadvantage for the detection of trace impurities, depending on the elements involved. For instance, the detection limit of Al-traces in Ta is much larger, if the sample is bombarded with Ar^+ instead of Xe^+ . However, for the detection of Ta-traces in Al, the use of Xe^+ will provide the higher sensitivity.

It has also been observed that use of Xe^+ increases the number and intensity of complex molecules and fragments, as well as of multiply-charged ions. This complicates the spectrum and is therefore, in general, not desirable, unless the additional peaks are needed for the identification of the material and for the calibration of the mass scale, and provided they do not interfere with the peaks of trace components of interest.

If the peak heights in the mass spectrum of any complex sample are divided by the sensitivity figures of Table I one obtains improved values of the concentration of the different constituents of the sample.

It was expected that the composition of the surface layer of an alloy would differ from the bulk material because of the different sputtering rates of the components. Under equilibrium conditions, all components would be sputtered in proportion to their bulk concentration and the ratio of bulk to surface concentration would be proportional to the sputtering rates. Before attaining this equilibrium condition, a change of the relative peak heights was expected to occur; however, this effect has not been observed. It must be assumed, therefore, if a transient condition exists, it persists for only a short time and equilibrium is reached before the first mass spectrum is recorded.

CHEMICAL TRACE ANALYSIS

Concurrently with the various phases of the contract during which the instrumental background was successively reduced and eventually eliminated, many tests were conducted to establish the sensitivity of the instrument for trace elements. Such tests included the analysis of Matthey's standard electrode rods of various metallic elements for optical spectroscopy and other NBS metal standards. In all cases, many impurity peaks were observed. Some of these corresponded to listed impurities, but their intensity was considerably larger than expected from the spectrographic analysis. Other peaks obtained with the mass spectrometer indicated the presence of elements which have not been detected at all by emission spectroscopy. The intensity of these background peaks was a reproducible characteristic for each particular sample, and, therefore, was not caused by instrumental background or by "memory effects".

Thus, the determination of the detection limit for trace impurities was seriously hampered by the complexity of the impurity content of spectrographic standards and the uncertainty of their impurity concentration. This difficulty is common for all types of mass spectrometers for solids and prevents accurate determination of the sensitivity of such instruments. However, a measure of the detection limit can be obtained in special cases with a substance containing an impurity which is separated on the atomic mass scale from other elements and whose concentration can be determined accurately by another independent method. A good example is a doped semiconductor, such as boron-doped silicon or antimony-doped germanium.

A series of tests was performed with boron-doped silicon either in the form of solar cells from the NASA, Goddard Space Flight Center (Dr. Fang) with the boron concentration varying as a function of depth from the surface, or, as homogeneous pellets, from the Dow-Corning Corporation, Hemlock, Michigan. The spectrum of silicon includes the isotopic peaks of $\text{Si}^+(28,29,30)$, $\text{Si}^{2+}(14,14\frac{1}{2},15)$, and $\text{Si}^{3+}(9\frac{1}{3},9\frac{2}{3},10)$. The spectrum of boron has its isotopic peaks at 10 and 11, the latter being the major peak. A measure of the sensitivity of the mass spectrometer for boron in silicon can then be obtained by measurements of the relative peak heights of B^{11} and Si^{28} for known concentrations of boron.

In current industrial practice, the concentration level of boron is determined by a resistivity measurement. This method is accurate up to 50 ppm. Above this concentration level, errors by about a factor of 2 are possible. Within this limit of uncertainty, however, a quantitative evaluation of absolute sensitivity of the mass spectrometer for boron in silicon is possible. Measurements of doped silicon pellets containing boron from 2000 ppm to 40 ppm have shown that the absolute sensitivity of the mass spectrometer for boron is independent of the boron concentration. The sensitivity is seven times

smaller for boron than it is for silicon. This linear response permits an accurate quantitative analysis of boron. A spectrum of silicon containing 40 ppm of boron is shown in Figure 15. For smaller concentrations of boron, the magnitude of the boron peak can no longer be measured accurately during a relatively fast single scan. The small arrival rate of boron ions at the first dynode of the electron multiplier is subject to considerable statistical fluctuations which makes it necessary to integrate over a sufficiently long time to collect an adequate number of ion pulses. This integration can be performed most conveniently with a Digital Memory Oscilloscope. The magnitude of a particular mass peak is recorded by repeated scanning over the peak and by adding automatically the output current as a function of the mass. The random noise is averaged by this method, but the signal amplitude increases above the detection limit. The storage process is monitored with an oscilloscope which also displays the final spectrum. Either photographing the oscilloscope display or recording the stored data with the X-Y recorder gives a permanent record. The spectrum in the vicinity of the B^{11} peak in silicon doped with 47 ppb of boron obtained in this manner is shown in Figure 16.

The concentration gradient of boron in a solar cell was measured over a thickness of 25 microns, as shown in Figures 17 and 18. The primary beam penetrates slowly deeper and deeper into the sample and the continuously recorded peak height at mass 11 represents a profile of the boron concentration distribution. Since the peak height changes continuously with time, it was not possible to use the integration method. Therefore, the detection limit was in the parts per million range. The calibration previously obtained from homogeneous silicon samples with known boron concentration has been used to convert the observed peak heights into actual boron concentrations.

A conventional spectroscopic standard consisting of spectroscopically pure graphite with a measured amount of a few carefully chosen trace elements can also be used for calibration. At no point on the atomic mass scale should their dissociation products or their multiply-charged ions overlap. This condition is well satisfied for most elements in Groups I, IIIA, and V of the periodic table. The other groups require restrictions to fewer elements if overlaps are to be prevented.

Before meaningful calibrations with graphite standards can be made, it is necessary to check the purity of this matrix. The graphite chosen is type SP-1 of the National Carbon Company of Union Carbide, Laboratory Number 90. Table II shows that only Mg, Al and Si had been detected by emission spectroscopy. However, the sputter source mass spectrometer showed a large number of additional peaks (Figure 19). Because of this discrepancy, the material was also analyzed independently by two outside laboratories with neutron activation. This method is very well suited to the present analysis since carbon does not become active and does not have to be separated chemically. Only Na and Cl were detected by this method, but the results for Na from the two laboratories differed by more than an order of magnitude. It should be mentioned

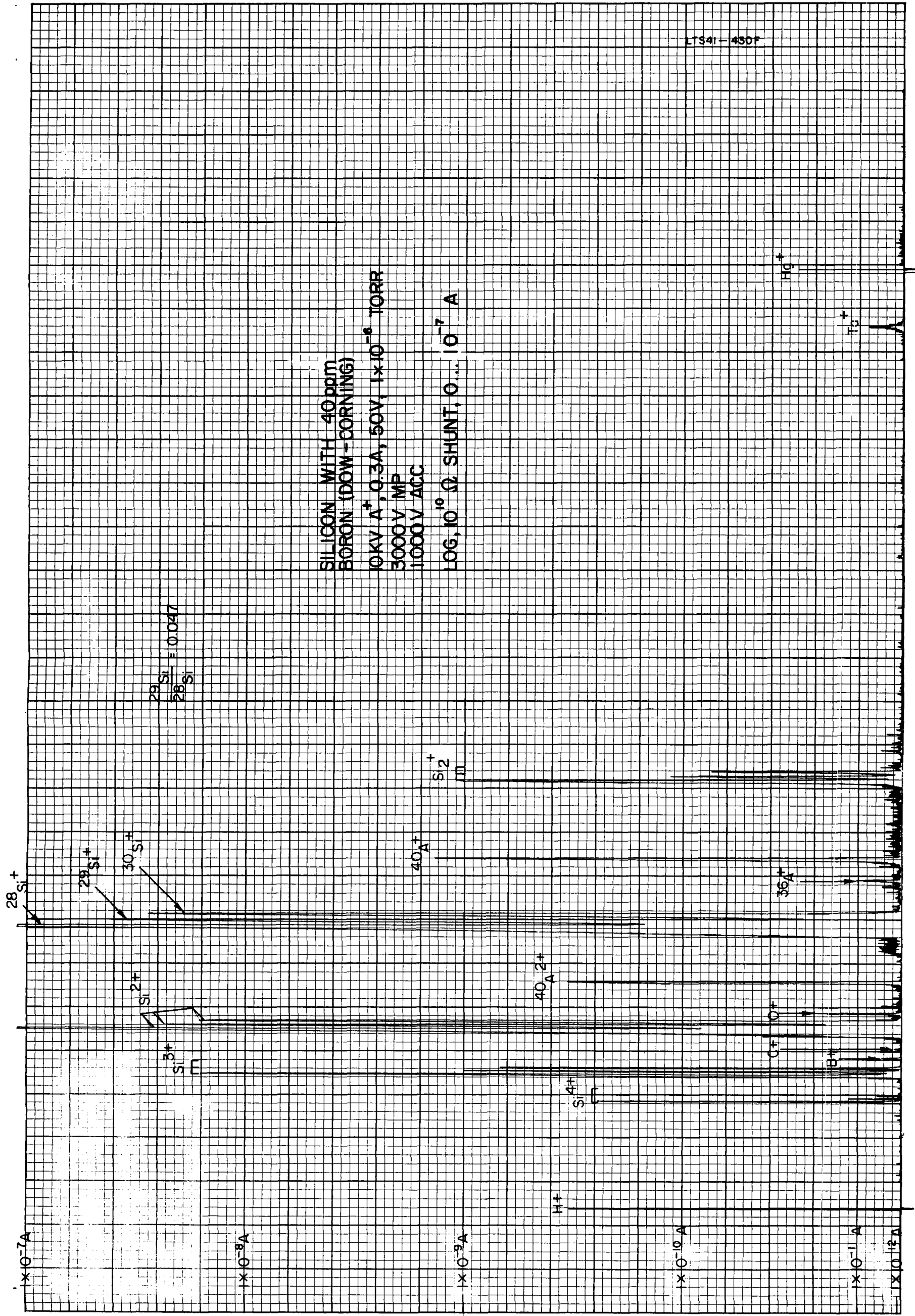


Figure 15. Spectrum of silicon doped with 40 ppm of boron (logarithmic peak amplitude scale).

ITS41-440F

SILICON WITH 47 ppb BORON (DOW-CORNING)

10KV A⁺, 0.3A, 50V, 1×10^{-6} TORR

3500V MP

1000V ACC, 20% SWEEP

LIN, 100MV, $10^6 \Omega$, ENHANCETRON

SWEEPTIME 16 sec,

INTEGRATION TIME 1 hour

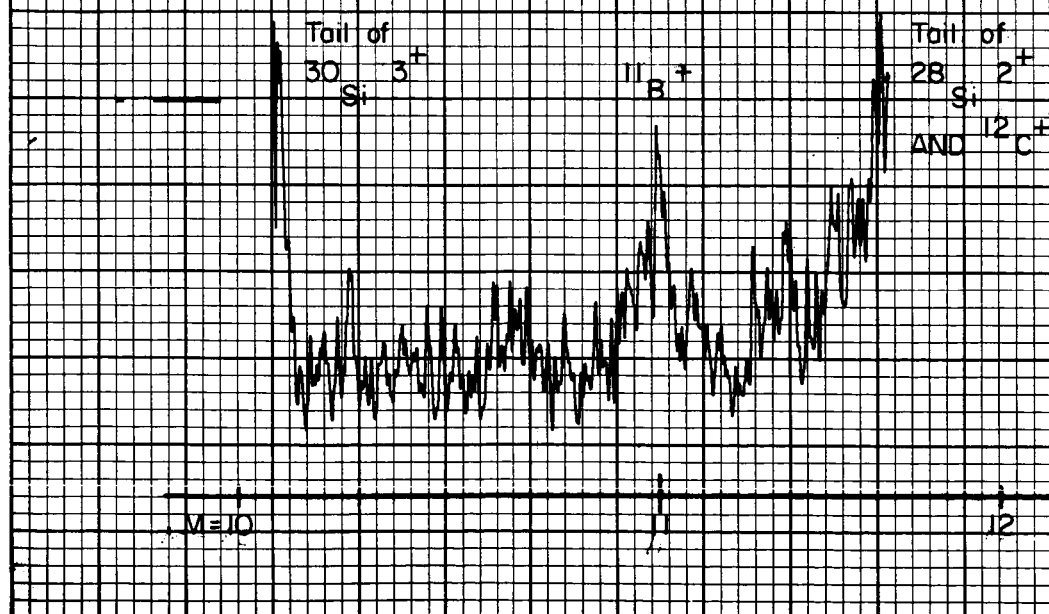


Figure 16. Spectrum of silicon doped with 47 ppb of boron (linear peak amplitude scale).

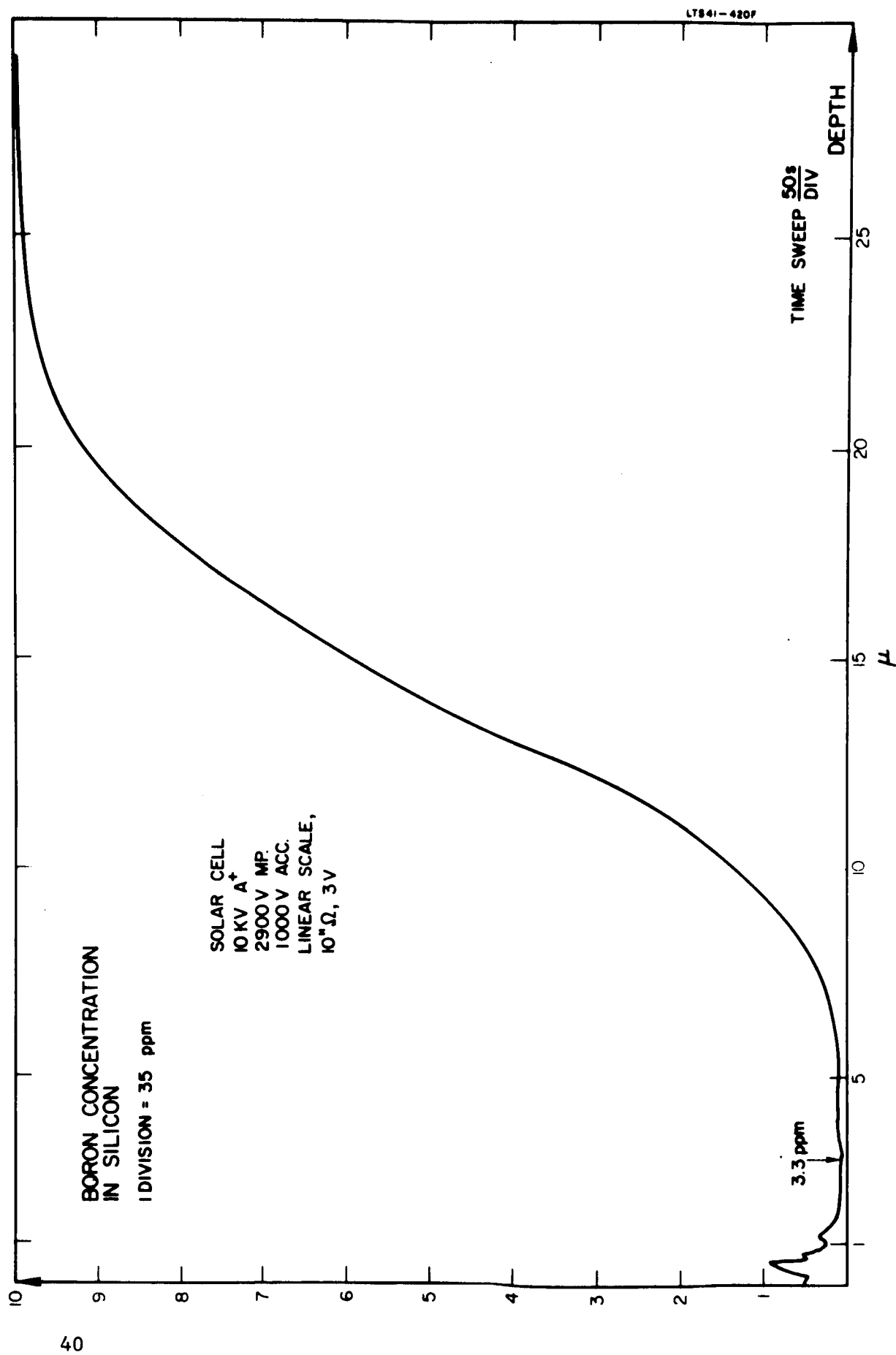


Figure 17. Boron concentration in silicon (solar cell).

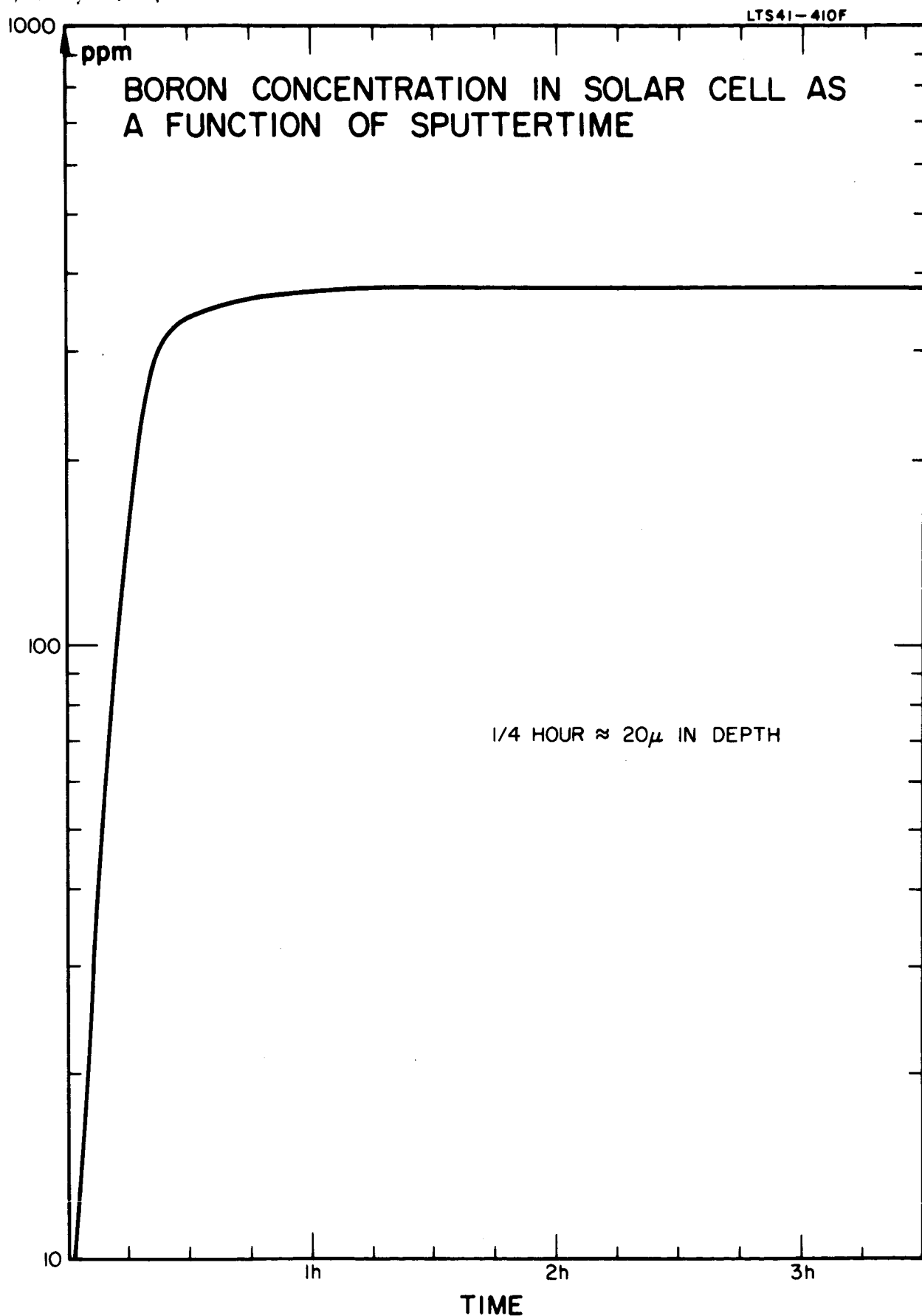
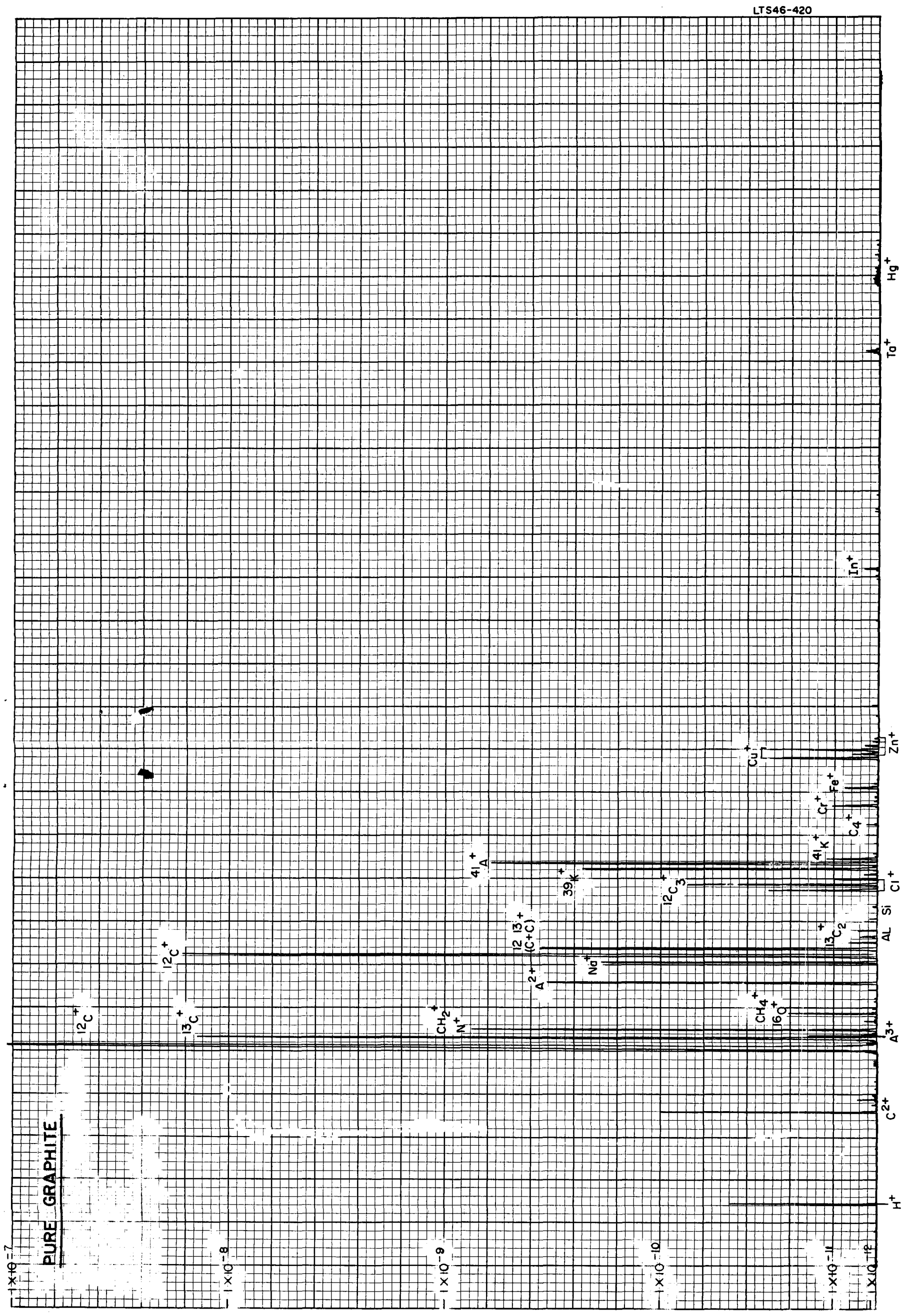


Figure 18. Boron concentration vs sputtering time (solar cell).



K&M 5 X 5 TO THE 1/2 INCH 358-6L
KEUFEL & ESSER CO.
MADE IN U.S.A.

Figure 19. Spectrum of spectroscopically pure graphite (logarithmic peak amplitude scale).

TABLE II
ANALYSIS OF GRAPHITE POWDER SP-1

Element	Emission Spectro- scopy ppm Atomic	Neutron Activation ppm Atomic		Sputter Source Mass Spectrometry current ratio ppm
		Union Carbide	General Atomic	
H				29
O				13
Na		4.3	0.34	150
Mg	0.05			Masked by C ₂ ⁺ peak
Al	0.1			1
Si	0.08			1
Cl		19.0	9.0	26
K		< 0.3	< 0.08	190
Cr		< 0.014	< 0.08	8
Fe			< 2.9	6
Cu				29
Zn		< 0.13	< 0.14	9
In		< 0.007	< 10 ⁻⁴	1

that the elements found by emission spectroscopy were not found by neutron activation analysis, and vice versa. The neutron activation data for the elements other than sodium and chlorine in Table II indicate that the presence of those elements in the graphite matrix was below the detection limit of the method. It is obvious that the sputter-source mass spectrometer is the more sensitive detector of trace impurities. Quantitative evaluation of the current ratios in terms of the actual concentrations would require an individual calibration, which has not yet been performed. It is also obvious that the quantitative results of the two other analytical methods, emission spectroscopy and neutron activation are not reliable. In view of this result, it became clear that the graphite matrix was unsuitable for the calibration with Na and K as originally planned. However, a graphite matrix with an appropriate selection of other elements would provide an acceptable standard for calibration.

The analysis of a pure platinum sample showed quite unexpected results that demonstrated the uncertainty of current analytical methods for trace impurities. The sample was a single crystal, purchased from Semi-Elements, Inc., Saxonburg, Pennsylvania. According to the manufacturer, it contained no detectable impurities; the total impurity content was estimated to be below 1 part per million. A mass spectrum of this sample (Figure 20) as obtained with the sputter-ion source contains large peaks of Al, Ca and Zr and smaller peaks of many other elements. Because the purity of the sample appeared questionable, other types of analysis were carried out. Emission spectroscopy, performed by the Jarrell-Ash Company, Waltham, Massachusetts, only showed extremely faint lines of Al, Si, Fe and Ag, suggesting a concentration of these elements below one part per million. A neutron activation analysis performed by the Union Carbide Corporation, Tuxedo, New York, did not show any impurities. However, only a few elements can be detected by neutron activation, even then the detection limits are high: Al, 14 ppm; Cu, 49 ppm; Ni, 40 ppm; Ga, 0.14 ppm; Zr, 1900 ppm; Rh, 114 ppm; Hf, 0.9 ppm atomic. The main difficulty with this particular sample arose because platinum becomes highly active during neutron irradiation and must be separated chemically from the impurities before they can be detected. This separation is difficult to perform since platinum is dissolved so slowly that most of the activated impurities decay before the separation is complete.

Two other promising analytical methods have not yet been applied to the platinum sample. The first, X-ray emission spectroscopy would be suitable for the detection of impurity levels of about 10 ppm above mass number 22 (Ti). This might just be adequate for some of the impurities. However, the sensitivity of this method is very poor for elements with lower mass number. Better sensitivity can be obtained generally by colorimetric and fluorimetric methods; however, the compatibility with a platinum matrix has yet to be investigated.

The second method, spark-source mass spectrometry is still the most sensitive and straightforward despite severe limitations in the quantitative interpretation of the data. Therefore, it was of great interest to us to

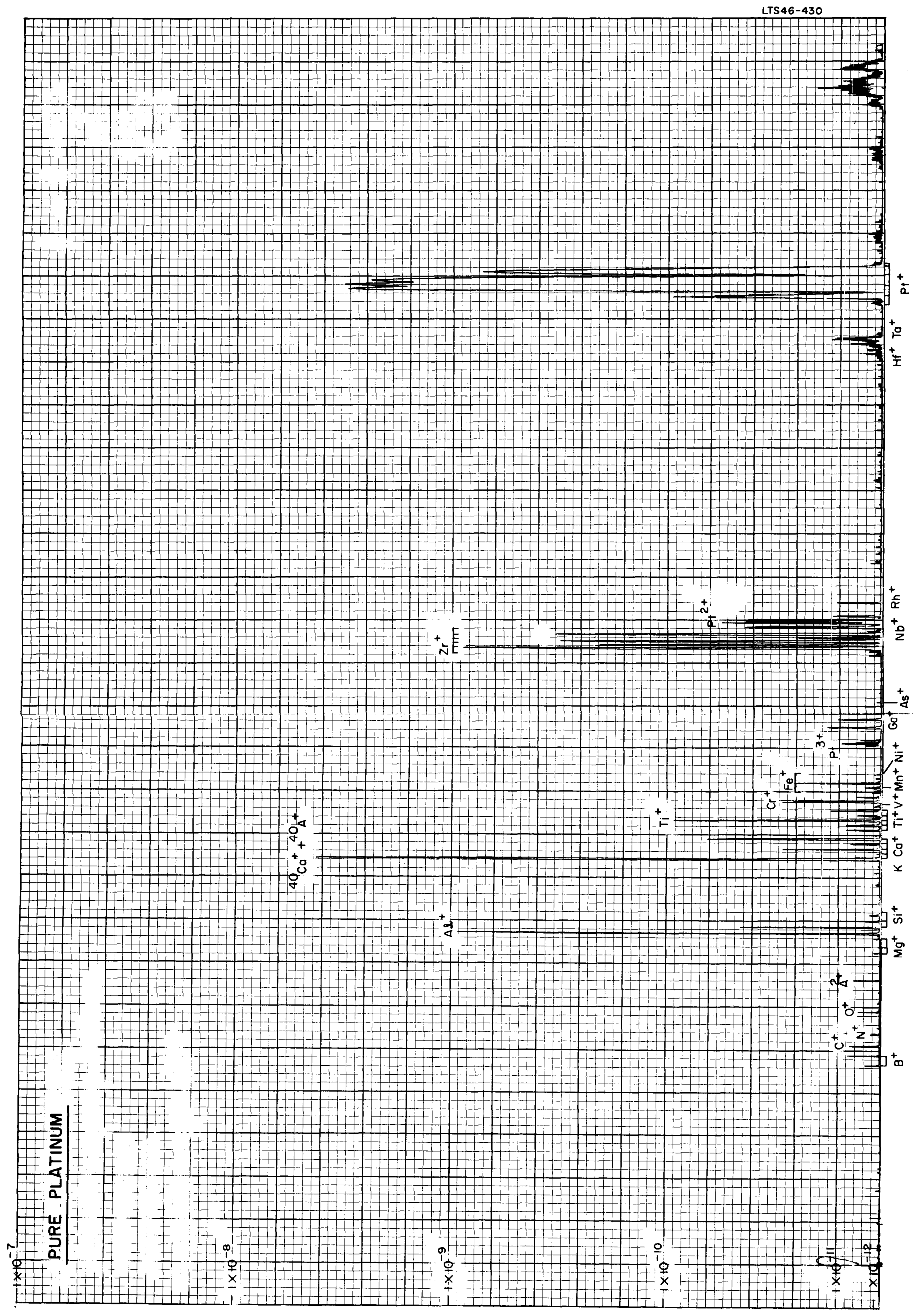


Figure 20. Spectrum of spectroscopically pure platinum (logarithmic peak amplitude scale).

obtain an analysis of the same platinum sample made on a standard CEC spark source mass spectrograph.* The figures given in Table III were obtained on the assumption of equal ion production for all elements in the spark source and for equal transmission through the analyzer. However, corrections for the sensitivity of the photographic plate have been applied. Comparison with the neutron activation detection limits shows higher impurity concentrations for Al, Ca, Ni and Ga by a factor of 3, 27, 10 and 35 respectively. The right column in Table III shows the results obtained with the sputter-ion source. The figures given represent the actual uncorrected multiplier output current ratio of the impurities to platinum. The sum of the peak heights of all isotopes of each element has been used for this purpose. A comparison between the two mass spectrometer measurements shows that the qualitative agreement generally is good since most elements were detected with both methods. One of the few exceptions is Ni which is a strong line in the spark source spectrum and hardly visible in the sputter source spectrum. The speculation that Ni is released by erratic sparking to the stainless steel sample holder of the spark source is not supported by the relative ratio of Ni to Fe and Cr. Quantitatively the agreement between the two methods, spark source and sputter source is poor. It is commonly assumed that in a spark source mass spectrometer the relative sensitivity for different elements is within one order of magnitude. However, exceptions to this rule are quite possible and the platinum matrix may be one of them. The relative sensitivity of the sputter-source mass spectrometer for different elements varies over a wider range, as can be seen from Table I, and it always requires an individual calibration to evaluate the spectra. For some elements the sensitivity is extremely high: Na, Al, K, Ca and Zr. For the analysis of these and probably some additional elements the sputter source is extremely well suited.

It should be mentioned that the platinum sample was analyzed repeatedly following a variety of other materials, and the results of the platinum analyses were reproducible. The samples analyzed before and after the platinum sample did not show the impurities of the platinum at all, or only with an intensity many orders of magnitude lower. It must, therefore, be concluded that these materials were really present in the sample and not introduced by the instrument. The peaks of Al, Ca, and Zr are so high that even 1/1000 of their intensity can easily be seen. If the emission-spectroscopic analysis is correct and the concentration of these elements is less than 1 ppm, then the solids mass spectrometer has a sensitivity better than one part per billion for these particular elements in a platinum matrix. This combination of materials seems to be very favorable for the detection of trace impurities. However, it cannot be generalized that this detection limit will be reached for all trace impurities.

* We wish to thank Dr. E. B. Owens of the Lincoln Laboratory of the Massachusetts Institute of Technology for testing this sample and for his careful evaluation of the mass spectrum.

TABLE III
ANALYSIS OF A PLATINUM SINGLE CRYSTAL

Element	Detection Limit Neutron Activation ppm Atomic	Spark Source Mass Spectrograph ppm Atomic	Sputter Source Mass Spectrometer current ratio ppthousand
B		present	1
C		present	.8
N			.1
O		300, not uniform	.5
Na		35	not visible
Mg			.1
Al	< 14	40	113
Si		present	43
P		present	not visible
Cl		5	not visible
K		20	.05
Ca	< 49	1300	340
Ti		not visible	14.7
V			.1
Cr		10	2.7
Mn		8	.2
Fe		150	1.9
Ni	< 40	400	.1
Cu		10	not visible
Zn		10	not visible
Ga	< 0.14	5	2.6
Ge		5	not visible
As		2	.05
Zr	< 1900	15	210
Nb		not visible	2
Rh	< 114	100	1
Pd		40	
Ag		20	not visible
In		30	
Sb		15	
Te		30	
Hf	< 0.9	plate foged	2.3

LITHIUM ISOTOPE ABUNDANCE DETERMINATION OF THE HOLBROOK METEORITE*

An important application of the solids mass spectrometer is the analysis of extra-terrestrial material. In particular, the determination of the abundance ratio of the isotopes Li^7/Li^6 in meteorites has been of great interest in connection with the nuclear synthesis of the light elements. Shima and Honda⁽¹⁾ have found a value of 10.5 for three chondrites; this ratio is slightly below the value of 12.0** found for terrestrial rock samples under the same experimental conditions. More recently Krankowsky and Mueller⁽²⁾ have found that meteoritic and terrestrial Li^7/Li^6 isotope ratios do agree within 2%.

The solids mass spectrometer was used for several measurements of the Li^7/Li^6 ratio on a small portion (about 0.4 g) of the Holbrook meteorite, which was chipped off from a larger fragment. Although the investigation is still in progress, the preliminary results appear to be sufficiently important to justify inclusion in this report. As indicated in a previous section, the basically new feature of the present instrument is its ability to analyze the bulk material without any chemical preparation.

Since the primary ion beam is focused to a small spot of only about $1/10 \text{ mm}^2$ area it is possible to analyze such small areas of the sample. By moving the sample relative to the beam one obtains a picture of the distribution of any particular element. It was found that the meteorite material is extremely inhomogeneous: some areas do not contain any detectable amount of Lithium, others contain relatively large amounts, well above 100 times the detectable minimum. It seems that the average Li content of 1-2 ppm, which has been measured by others, is mainly the result of a few small areas of relatively high concentration; between these areas the concentration of Lithium is very low. The inhomogeneity of the sample supports the hypothesis that meteorites are conglomerates of materials of quite different origin.

The measurements of the Li^7/Li^6 ratio were performed only at locations which are rich in Lithium. Even under these conditions, the output signal at the mass spectrometer ion collector was rather small and required integration over several minutes to provide sufficient accuracy in the presence of the statistical fluctuations. For this purpose, the two peaks at mass 6 and 7 were scanned repeatedly at a speed of twenty seconds per scan and the results of fifty such scans were averaged by means of a Digital

* The investigation was undertaken at the suggestion of Dr. E. L. Fireman of the Smithsonian Astrophysical Observatory, who also provided a sample of the Holbrook meteorite.

**

These figures, as well as the following, are the ratios of the mass-peak heights without any correction for mass discrimination.

Memory Oscilloscope.* The results of six different measurements are: $\text{Li}^7/\text{Li}^6 = 9.5, 27.9, 16.9, 21.3, 19.0, 15.1$. (See Figure 21 left side.) The astonishing result is that such very large variations of the Li^7/Li^6 ratio do occur. The actual variations are probably even larger since during the 1000 seconds used for each measurement, the primary ion beam penetrates about 20 microns into the sample and any variation with depth is averaged out. The first three measurements were performed at the same spot with increasing depth, the others at different spots. For each measurement, about 5×10^{-6} g of the meteorite material was consumed containing less than 10^{-9} g of Lithium.

According to the theory of W. A. Fowler et al.⁽³⁾ about the formation of the light elements, it is assumed that originally the same number of Li^6 and Li^7 nuclei were produced by high energy spallation reactions and that the present deviations from the original ratio, $\text{Li}^7/\text{Li}^6 = 1$, are the result of different neutron reactions, primarily the reaction $\text{Li}^6(n, \alpha) \rightarrow \text{T}^3$, which has consumed most of Li^6 and increased the ratio Li^7/Li^6 . The large variations of this ratio, which was observed, indicate that the small particles which comprise the meteorite were exposed to different amounts of neutron radiation. Perhaps, the particle with the low ratio 9.5 spent a considerable time in the interior of a larger body, where it was shielded from the neutron flux, whereas the particles with the high ratio were located near the surface. It may be assumed that this larger body was broken up in a collision and that the small particles recondensed to form the meteorite.

In order to check this result it was decided to repeat the measurement with a terrestrial sample which produces a Lithium peak of about the same intensity. The results from Hornblende are: 12.05, 12.57, 12.53, 10.75, 11.39, 11.32. (See Figure 21 right side.) It is obvious that these variations are much smaller than those found on the meteorite. Further measurements will be necessary to decide whether these relatively small variations on the terrestrial material are genuine or caused by statistical fluctuations of the small Li ion current. Measurements on pure metallic Lithium, where the ion current was high, gave quite consistent results which varied by less than 1%. In this respect, the sputter-ion source was far superior to the customary thermionic source where the Lithium peak height ratio increases by about 10% within a few hours after a new sample has been introduced.

Since the work was concentrated on Lithium, only one mass spectrum was obtained over a wider mass range. From the intensities of Mg^{24} and Si^{28} , singly, doubly, and triply charged, it was possible to exclude the possibilities of interference of Li^6 by $\text{Mg}^{24,4+}$ and of Li^7 by $\text{Si}^{28,4+}$. It should also be mentioned that on this particular spectrum a fairly large peak at mass 11 was

* Nuclear Data, Inc., ND-800 Enhancetron 1024.

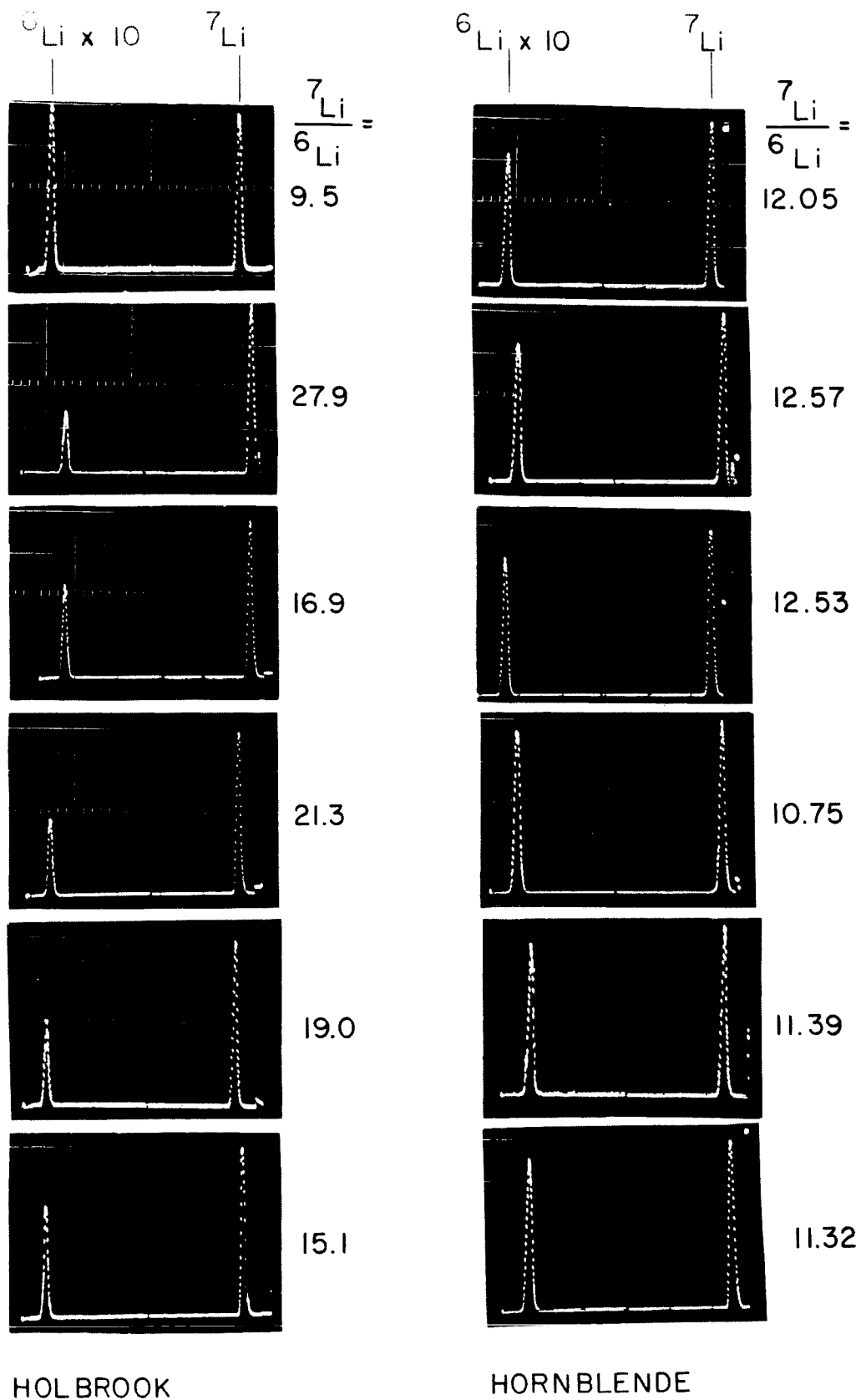


Figure 21. Li-isotope ratio for Holbrook and Hornblende.

present which we attribute to B^{11} . However, there was no trace of B^{10} which should be present with an intensity of about 25% of B^{11} . It is possible, but not likely, that the B^{10} peak was absent because of statistical fluctuations of the small current and the short time of the scan over the peak. However, it is more likely that the process $B^{10} (n, \alpha) \rightarrow Li^7$ actually took place and has depleted B^{10} and enriched Li^7 as it has been proposed by Fowler et al. (4) Before such a statement can be made with certainty it will be necessary to measure the Boron isotopes with the same accuracy as the Lithium isotopes, to correlate the location of these and other elements in the meteorite, and to extend the measurements to other meteorites.

MINIATURIZATION OF THE SOLIDS MASS SPECTROMETER FOR A LUNAR MISSION

The laboratory mass spectrometer described previously which is shown in Figure 22 was designed for maximum sensitivity without particular regard to weight and power. Even so, it is considerably more compact than spark-source spectrometers of comparable performance. Clearly, however, it is not suitable for space applications in its present form (78 cu. ft, 2000 lb, 4000 watts).

The approach to miniaturization can take two forms:

(1) The smallest instrument for lunar application with the same performance as that of the laboratory instrument.

(2) The performance of a scaled-down instrument compatible with spacecraft requirements.

It can be shown that in the former case, the instrument would be 6 cu. ft, 200 lbs, and require 2000 watts. This is considerably beyond the capability of early lunar probes, and we are compelled to confine ourselves to the latter approach, where a realistic design objective appears to be an instrument of at most 1 cu ft, weight 30 lb, requiring 30 watts.

These conclusions arise from the following considerations: if the same resolution and sensitivity as in the laboratory device are to be obtained, then only minor changes can be made in the duoplasmatron ion source and in the mass analyzer. Use of lighter structural materials will result in little weight reduction since most of the weight is due to the electromagnet. Any weight reduction obtained by replacing stainless steel parts by aluminum or aluminum alloy will probably be made up by the severe structural requirements to withstand shock and vibration and to prevent misalignment of the electric and magnetic field adjustments which are critical for both resolution and sensitivity.

The only major simplifications which are possible in the lunar instrument without loss of sensitivity and resolution are the elimination of the vacuum pumps and the miniaturization of the electronics. Elimination of the vacuum pumps results in reduction of bulk, weight, and power consumption, as does miniaturization of the electronics. However, there remains the power consumed by the electromagnet in the analyzer which cannot be replaced by a permanent magnet without limiting the mass range of the instrument, as discussed in more detail later on.

As already indicated, these modifications reduce the volume by a factor of 13, the weight by a factor of 10 and the power by a factor of 2, but they do not go far enough. Some limitations in performance have to be accepted in return for drastic reductions in volume, weight, and power consumption.

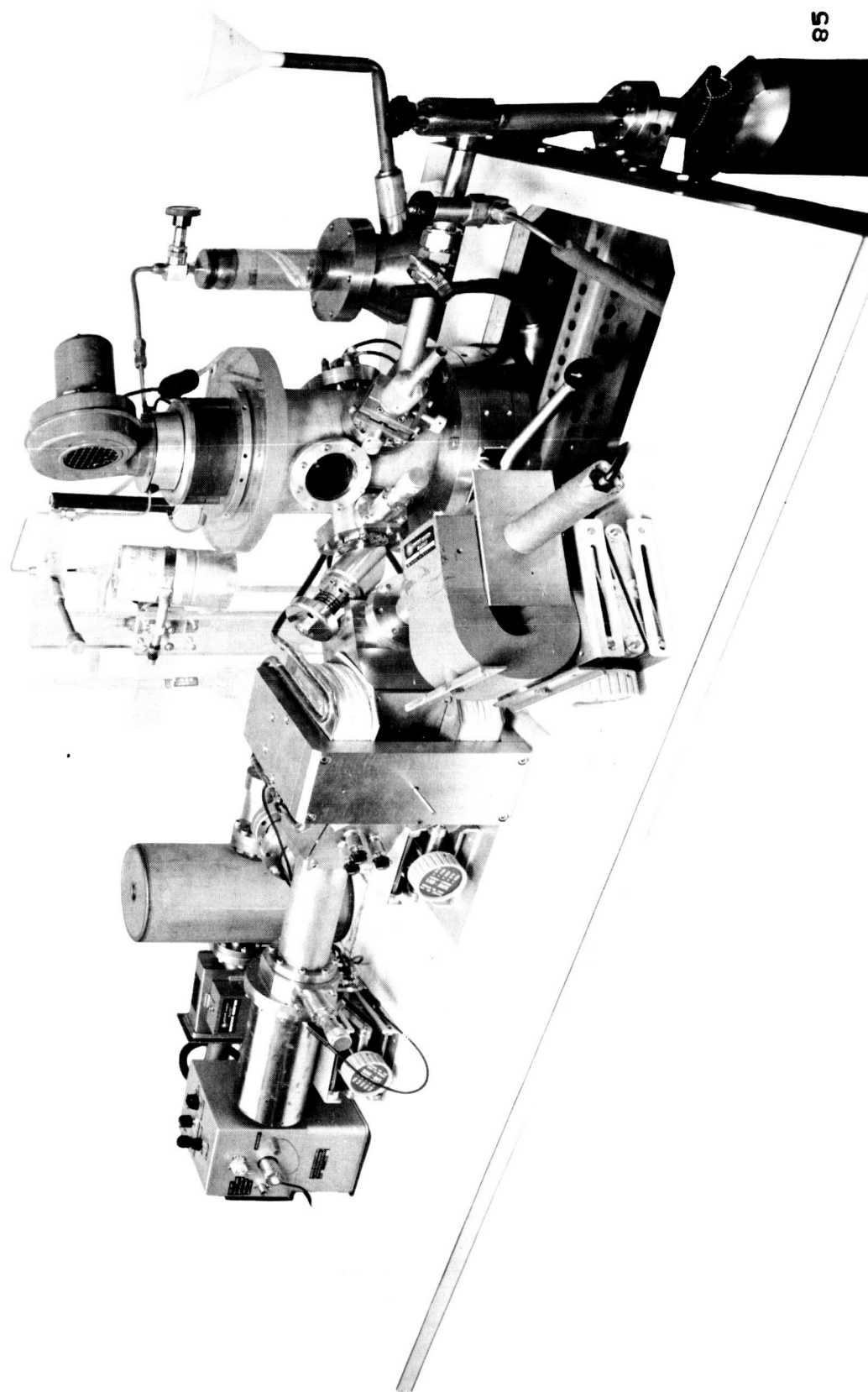


Figure 22. Laboratory model of solids mass spectrometer.

Ion Source

A major disadvantage of the duoplasmatron ion source is its hot filament which requires about 100 watts: its limited life entails some risk regarding instrumental reliability. The proposed instrument will, therefore, use a cold-cathode ion source which is burnout proof and whose power consumption is negligible in comparison. However, the useful ion beam current density is smaller, and will thus lower the sensitivity of the mass spectrometer.

Analyzer

Miniaturization of the analyzer without sacrifice of resolution requires that the slits be reduced proportionally. For example, a linear reduction by a factor of $1/2$ will reduce the weight to $1/8$ and the slit area and transmission to $1/4$ or even less if the image errors can not be neglected. A more serious intensity loss is caused by the fact that the radius of the orbit in the magnetic field has also to be reduced by $1/2$, which requires that the acceleration voltage has to be reduced to $1/4$ if the magnetic field strength is kept constant. This intensity loss will be more serious in the upper part of the mass range where the accelerating voltage is low, even before the reduction in size. From previous experimental experience, it can be assumed that reduction to half size will reduce the output current by about one order of magnitude. Since the output current of the present mass spectrometer is high enough to detect some impurities in the parts per billion range, it can be expected that the miniaturized instrument will still have enough sensitivity to measure all major constituents and to detect the more abundant impurities. It is believed that this aim is adequate for early surveyor flights. The development of a more sensitive instrument for special purposes, such as age determination, should be postponed until the major composition of the moon is known and until the weight limitations of such an instrument can be relaxed. In the light of considerable experience with a magnetic analyzer, successful operation of this type of mass spectrometer with a cold-cathode ion source and a permanent magnet can be predicted with confidence.

Magnet

For reduced power consumption, a permanent magnet appears preferable to the present electromagnet. However, the use of a permanent magnet results in difficulties of scanning over a wide mass range. Variation of the magnetic field with a motor-driven shunt seems to be feasible; however, the power consumption of the motor and the questionable reliability are serious drawbacks. Electric scanning over a small mass range is preferable although it will cause a moderate amount of mass discrimination, which can be determined during the calibration tests. However, a larger mass range (1-100) can not be covered by this simple method since the acceleration voltage would be either too low

for the heavy masses or too high for light masses. The transmission of the analyzer and the sensitivity of the instrument would be severely diminished if the acceleration voltage is reduced below 500 volts. On the other hand, insulation difficulties will start at about 5000 volts. Within these voltage limits a mass range of one order of magnitude can be covered. This is adequate for the expected major lunar constituents Si, Al, Fe, Mg, Ca, Na, K which are all within the mass range 23 to 58. If an acceleration voltage of 1000 volts is chosen for mass 58 then mass 23 requires 2500 volts. A scanning mass spectrometer for only this limited mass range can be made very light and reliable. Since it can provide information of great interest about the basic composition of the moon's surface, it is recommended for the early surveyor flights.

For later flights, it will be desirable to extend the mass range. Most of the above-mentioned elements will be present as oxides, but perhaps some will be in the form of hydroxides, carbonates and chlorides. Information regarding the existence of these compounds on the moon is important, since it might open the possibility to produce such life-supporting materials as oxygen and water from lunar minerals. An upward extension of the mass range is necessary to cover these heavier molecular ions and a downward extension to cover the fragment ions C, O, OH and OH₂. In addition, the light masses H, D and He are of great scientific interest since these gases are the main constituents of the solar wind. It is possible that during the prolonged exposure of the lunar surface large amounts of these gases have become absorbed there. An extension of the mass range down to mass 1 and up to at least mass 80 would therefore be desirable.

In order to extend the mass range it is proposed to use three ion collectors. These will be located in different positions relative to the magnetic field, such that the three mass ranges covered by them overlap slightly.

A double-focussing mass analyzer which is suitable for simultaneously supplying more than one ion collector was first designed by Mattauch and Herzog⁽⁴⁾ and has been recently adapted to space research by E. B. Meadows⁽⁵⁾ together with Hall, Howden and Iwasaki.⁽⁶⁾ The final version of this instrument has been described by Spencer and Reber.⁽⁷⁾ Since this instrument has already been flown successfully in the Explorer 17 satellite for the measurement of atmospheric constituents from mass 4 (He) to mass 32 (O₂), it represents a good starting point for the design of a flyable solids mass spectrometer. The mass analyzer of this instrument has six ion collectors which are permanently tuned to the masses 4, 14, 16, 18, 28, 32. Since the electrometer can be switched from one collector to the next scanning is performed at constant voltage and magnetic field. This instrument weighs 12 lbs and its power consumption is 20 watts.

This analyzer can easily be combined with a sputter-ion source for solids to analyze the lunar surface. Two versions are promising:

A.) A simple instrument with seven ion collectors, in fixed positions, permanently tuned to the main peaks of the major constituents: 23 (Na), 24 (Mg), 27 (Al), 28 (Si), 39 (K), 40 (Ca), 56 (Fe). Advantages of this instrument over the single range scanning spectrometer mentioned earlier are: 1) Simpler telemetry, since only the peak heights and not the peak shapes have to be transmitted, and also, because switching between the collectors is quite slow (8 seconds for each collector). 2) The charge on each collector can be accumulated over the whole sweep time of 56 seconds, which eliminates the need for electron multipliers. The disadvantages are: 1) Other elements can not be detected, even if present in large amounts. 2) All data may be lost if the tuning of the instrument is disturbed slightly by shock or by extreme temperatures. The scanning instrument described before is free of these drawbacks.

B.) A more sophisticated instrument with three exit slits and three electron multipliers, and with electric scanning. The three outputs would cover the overlapping mass ranges 1-8, 7.5-60 and 30-240. One telemetry channel is sufficient, if it is switched from range to range during successive scans.

The field arrangement of the double focussing mass analyzer mentioned previously is not well suited for this purpose, because extension of the mass range from mass 32 to 240 requires a magnetic field 2.7 times larger. This would increase the weight seven-fold which is considered prohibitive for a lunar flight instrument. Other field arrangements do not require such a heavy magnet. Figure 23 is a rough sketch of such a basic instrument shown in full size. This mass spectrometer was computed on the basis of the "General Theory of Double Focussing Mass Spectrometers" developed by R. Herzog and P. Hauk.⁽⁸⁾ The magnet for this arrangement will have the same field strength (3500 gauss) and approximately the same weight as that flown by Spencer and Reber. The exit edge of the pole piece is almost straight but does not project through the entrance point. The deflections of the electric and magnetic field are in the same direction, similar to the instrument of Bainbridge and Jordan.⁽⁹⁾

The primary ion beam is generated in a Penning type, cold cathode ion source 1 and focussed by the lens system 2 onto the sample 3. Secondary ions are drawn off from the sample by the lens system 4 and concentrated on the entrance slit 5. The beam is deflected in the electric field 6 and in the magnetic field 7 and focussed on the exit slits 8, 9, and 10. Behind each exit slit is either a separate electron multiplier or a detection system as described by Daly⁽¹⁰⁾ consisting of an ion-electron converter, a plastic phosphor and a photomultiplier. The plastic phosphor and the multiplier can be replaced by a P-N junction as described by White et al.⁽¹¹⁾ The exit slits are located at the positions of the images of the entrance slit produced by different masses. Slit 8 would cover the mass range 1 to 8 if the acceleration

LTS43-1105

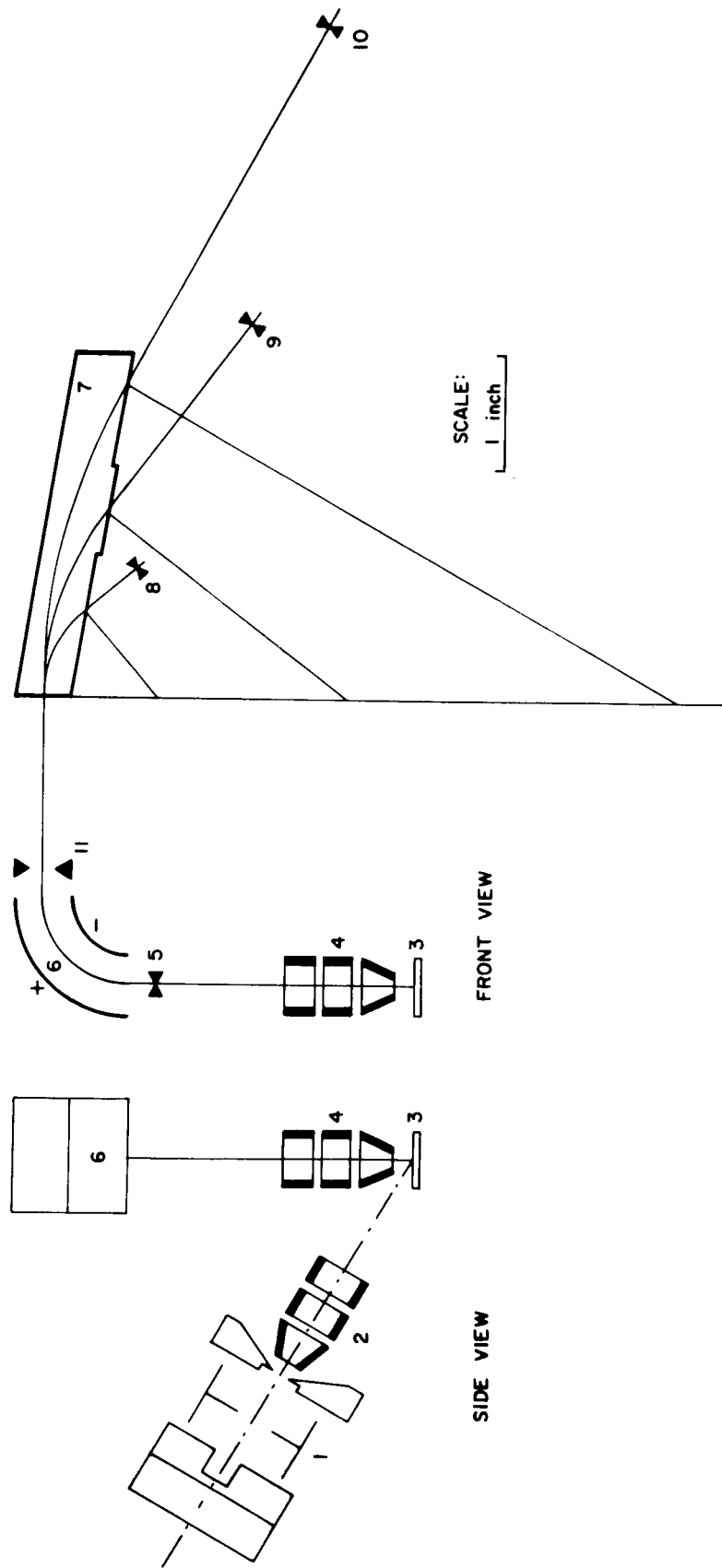


Figure 23. Proposed flight design of solids mass spectrometer.

voltage is swept over from 4000 to 500 volts. Under the same conditions slit 9 would cover the mass range 7.5 to 60 and slit 10 the range 30 to 240. The location of the slits 8, 9, and 10 is such that ions which leave the sample with different initial velocities are focussed (double-focussing spectrometer).

One characteristic feature of this field arrangement is that a real image of the entrance slit is located between the electric and magnetic field. The wide slit 11 at this position limits the velocity range to be focussed. The advantage of this instrument is that the velocity range is independent of the angular spread of the beam at the entrance slit and can therefore be better controlled.

The method to be used for exposure of lunar surface material to the bombarding beam depends on whether an instrument can be soft-landed on a sufficiently smooth and flat surface. In this case, it would only be necessary to provide a hole in a thin target plate which is lowered slowly until it touches the surface and the lunar material plugs the hole. Since there is no assurance that these conditions can be met, an alternative solution consists of a target holder which permits the introduction of powdered or granular material. It will then be sufficient to pulverize a small amount of lunar material for analysis - and to drop it on the target holder. No additional sample preparation is necessary. The target holder will also permit the introduction of terrestrial material of known composition for in-situ calibration of the instrument.

An instrument of type B will reliably yield maximum amounts of analytical data within moderate limits of size and weight.

REFERENCES

1. Shima, M. and M. Honda, J. Geophys. Res., 68, 2849, 1963.
2. Krankowsky, D., and O. Mueller, Geochmica et Cosmochimica Acta 28, 1625, 1964.
3. Fowler, W., J. Greenstein, F. Hoyle, Am. J. Phys. 29, 393, 1961.
4. Mattauch, J. and R. Herzog, Z.f.Phys. 89, 786, 1934.
5. Meadows, E. B., Eighth Annual Meeting of ASTM Committee E-14 on Mass Spectrometry, Atlantic City, 1960.
6. Hall, L. G., P. F. Howden, and T. F. Iwasaki, Eighth Annual Meeting of ASTM Committee on Mass Spectrometry, Atlantic City, 1960.
7. Spencer, N. W. and C. A. Reber, Space Research 3, 1151, 1963.
8. Herzog, R. and V. Hauk, Annalen der Phys. 33, 38, 1938.
9. Bainbridge, K. T. and E. B. Jordan, Phys. Rev. 50, 282, 1936.
10. Daly, N. R., Rev. Sci. Inst. 31, 264, 1960.
11. White, F. A., F. M. Rourke, J. C. Sheffield and L. A. Dietz, IRE Transactions on Nuclear Science NS-8, 13, 1961.